the spectra in 0 and 5% (v/v) are highly superimposable, both having a large negative band at 205-235 nm, typical of an α/β protein. This result shows that the protein does not undergo any detectable change in secondary structure following the addition of small quantities of TFE, even at a concentration able to induce aggregation. By contrast, the CD spectra acquired in 80% (v/v) TFE and in 5 M urea with no TFE indicate major changes in secondary structure composition under these conditions (Fig. 3.6).

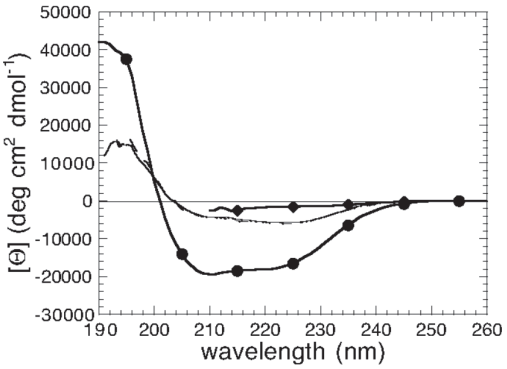

Figure 3.6 Far-UV CD spectra of AcPDro2 in 0% TFE (solid line), 5% TFE (dashed line), 80% TFE (circles) and 5M urea without TFE (diamonds).

The near-UV CD spectra are also highly superimposable when recorded for protein samples in 0 and 5% TFE (Fig. 3.7). The broad peak at 262-280 nm and the two sharp peaks at 286 and 295 nm are present in both spectra, indicating that no modifications in protein structure packing, particularly in anisotropy of aromatic residues, seem to occur following the addition of 5% TFE. By contrast, the near-UV CD spectrum of the protein sample denatured in 4.5 M urea, recorded as a control, shows that AcPDro2 has lost its native packing following denaturation (Fig. 3.7).

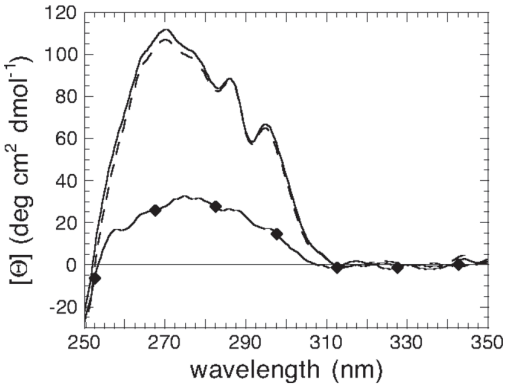

Figure 3.7 Near-UV CD spectra of AcPDro2 in 0% TFE (solid line), 5% TFE (dashed line)and 4.5M urea without TFE (diamonds).

Modifications in the chemical environment around tryptophan residues were also monitored with fluorescence spectroscopy (Fig. 3.8). AcPDro2 has two tryptophan residues at positions 42 and 68, respectively. The intrinsic fluorescence spectra of the protein in 0-5% (v/v) TFE are very similar to each other, as shown for the two representative spectra in 0 and 5% TFE (Fig. 3.8). We found no significant differences for the wavelength of maximum emission (λ_{max} = 350 nm) in 0-5% TFE. The weak increase of fluorescence emission from 0 to 5% TFE correlates linearly with TFE concentration (Fig. 3.8, inset); hence, it is most likely attributable to solvent effects rather than to a conformational change. On the other hand, the spectra recorded in 80% (v/v) TFE and 5 M urea with no TFE show a noticeable loss in total fluorescence emission and a red-shift of the λ_{max} value from 350 nm to 355 nm (80% TFE) and 358 nm (5 M urea).

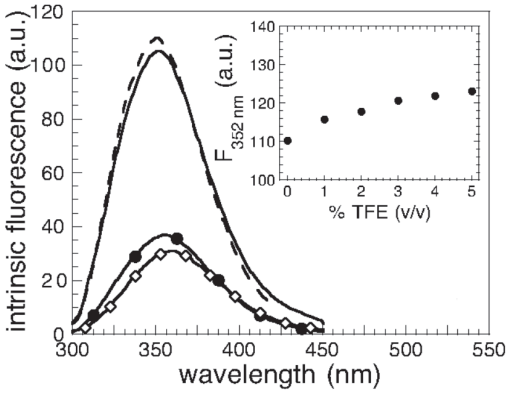

Figure 3.8 Intrinsic fluorescence spectra of AcPDro2 in 0% TFE (solid line), 5% TFE (dashed line), 80% TFE (circles) and 5M urea without TFE (diamonds). The inset shows the intrinsic fluorescence at 352 nm versus the percentage of TFE in the solution.

Possible variations in the solvent-exposure of hydrophobic clusters following the addition of TFE have been further investigated using ANS. This dye is known to bind to clustered hydrophobic residues that are exposed to the solvent in a protein and hence to give rise to a blue-shift and an increase in fluorescence emission intensity (120,136). Both the protein samples in 0 and 5% (v/v) TFE were found to cause very weak and very similar increases of

fluorescence emission of ANS (Fig. 3.9). The difference spectra, obtained in each case by subtracting the spectrum of free ANS from that recorded in the presence of protein, exhibit λ_{max} values of 480 and 490 nm for the protein in 0% and 5% (v/v) TFE, respectively, a blue-shift from the λ_{max} of 515 nm for free ANS (Fig. 3.9). This indicates that small fractions of ANS molecules are bound to the protein, both in 0 and 5% TFE. The weak peaks shown in the difference spectra may perhaps be attributed to the ability of ANS to bind to cationic groups of the protein (121), since at pH 5.5 AcPDro2 has a net charge of +6. However, the fact that a similar relative increase of ANS fluorescence is caused by the protein in the two conditions rules out that additional hydrophobic clusters become superficial following the addition of small amounts of TFE.

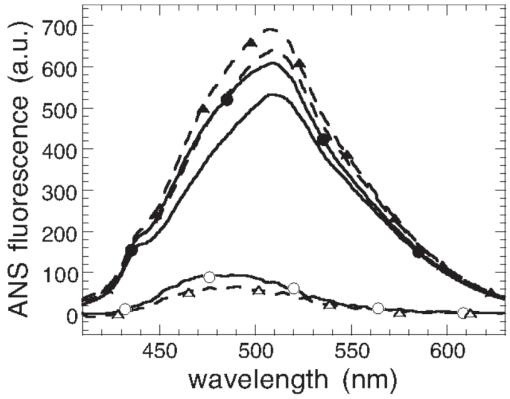

Figure 3.9 Fluorescence spectra of 55μM ANS in the presence of 0.02 mg ml^{-1} AcPDro2 in 0% TFE (solid line with solid circles) and 5% TFE (dashed line with solid triangles). Spectra of free ANS ain the absence of protein were also recorded as contols in 0% TFE (solid line) and 5% TFE (dashed line). Difference spectra, obtained by subtracting the ANS spectra recorded in absence of protein from the corresponding ones acquired in its presence, are also shown in 0% TFE (empty circles) and 5% TFE (empty triangles).

The acylphosphatase activity of AcPDro2 was also determined in the presence of low concentrations of TFE, ranging from 0 to 5% (v/v). The catalytic activity of acylphosphatases requires the correct spatial positioning of residues that are relatively distant in the sequence, namely Arg27, Asn45 and the residues of the loop ^{19}GRVQGV^{24} (95). We found that the ability of AcPDro2 to hydrolyse the acylphosphate bond did not change significantly within the range of TFE concentration tested (Fig. 3.10). Overall, the analysis presented

here indicates that the protein populated under aggregating conditions, but before aggregation occurs, has structural and catalytic properties indistinguishable from those of the native protein under conditions in which it resists aggregation.

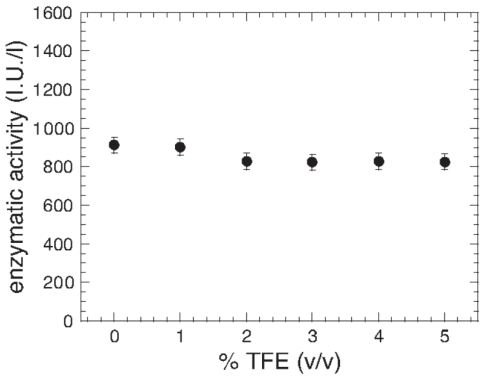

Figure 3.10 Enzymatic activity of AcPDro2, tested by adding the protein to a final concentration of 0.5 μg ml^{-1} to solutions containing 4mM benzoylphosphate. "I.U./I." indicates international units of activity per liter.

3.4 Absence of destabilization under aggregating conditions

Thermodynamic stability of native AcPDro2 has been monitored by equilibrium denaturation experiments carried out at TFE concentrations ranging from 0 to 5% (v/v). We followed unfolding of AcPDro2 at equilibrium using urea as a chemical denaturant and intrinsic fluorescence as a spectroscopic probe. Fig. 3.11a shows the unfolding curves normalised to the fraction of folded protein with and without 5% (v/v) TFE. The unfolding transitions appear to occur at similar urea concentrations and with similar cooperativities in the two solution conditions (Fig. 3.11a). The main thermodynamic parameters of the unfolding reaction were inferred at all TFE concentrations tested from the equilibrium curves assuming a two-state model and using the equation described by Santoro and Bolen (124). The free energy

change upon unfolding in the absence of urea ($\Delta G_{U-F}^{H_2O}$) and the midpoint of unfolding (C_m) were found to remain substantially unchanged at the different TFE concentrations used (Fig. 3.11b). We concluded that addition of up to 5% TFE does not lead to a substantial thermodynamic destabilisation of the native structure of AcPDro2.

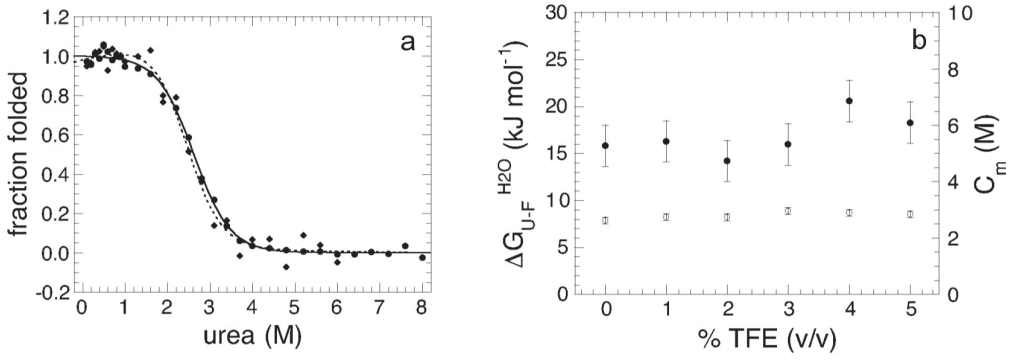

Figure 3.11 (a) Equilibrium urea unfolding curves of AcPDro2 in 0% (circles) and 5% (diamonds) TFE. The lines represent the best fit to the equation described by Santoro & Bolen (124), for 0% TFE (solid line) and 5% TFE (dashed line). (b) Variations in $\Delta G_{U-F}^{H_2O}$ (solid circles) and C_m (empty circles) with TFE concentrations. Error bars represent standard deviations.

Folding and unfolding kinetics of AcPDro2 were monitored using a stopped-flow device coupled to a fluorescence detection system. In a first set of experiments the folding and unfolding rate constants were measured at TFE concentrations ranging from 0 to 9% (v/v). In all cases folding was monitored after a ten-fold dilution of the protein denatured in 6 M urea to a reach a final urea concentration of 0.6 M. Two exponential phases were observed. The first phase, corresponding to the major folding phase, shows a marked positive dependence on TFE concentration and reaches the maximum rate at *ca.* 6-8% TFE (Fig. 3.12a, black circles). This behaviour is typical of all proteins studied so far and has been attributed to the fact that folding rate reaches a maximum

when the formation of secondary structure is optimal and close to native-like levels (137). The unfolding reaction was monitored by a ten-fold dilution of the native protein in solutions containing 6 M urea to reach a final urea concentration of 5.4 M urea. Unfolding appears to be a monophasic process in all recorded traces. The unfolding rate constant appears to have a strong positive dependence on TFE concentration, reaching no apparent maximum in the range 0-9% TFE (Fig. 3.12a, white circles). The unfolding and refolding traces have been fitted to single and double exponential functions, respectively, of the form:

$$y(t) = q + \sum_{i=1}^{n} A_i \exp(-k_i t) \qquad \text{(A)}$$

where $y(t)$ is the fluorescence at time t, q is the fluorescence value at equilibrium, A_i and k_i are the amplitude and rate constant of the ith phase, respectively, and n is the number of observed phases.

In a second set of experiments the folding and unfolding rate constants were determined in 0 and 5% (v/v) TFE in the presence of various urea concentrations: the unfolding and folding kinetics were monitored at final urea concentrations ranging from 1.80 M to 7.20 M for unfolding and from 0.50 M to 3.20 M for folding. The natural logarithm of the folding and unfolding rate constants obtained from fitting measurements to Equation (A) was plotted versus urea concentrations. The resulting chevron plots are showed in Fig. 3.12b for both the analyses carried out in the presence and absence of 5% TFE. In 5% TFE the chevron plot is characterised by a noticeable downward curvature at 0-0.6 M urea, indicating that the major fast phase for folding has a decreasing dependence on urea concentration as the latter decreases. This

phenomenon is often referred to as a roll-over and probably reflects the accumulation of a partially folded or misfolded state during folding at these low urea concentrations (138).

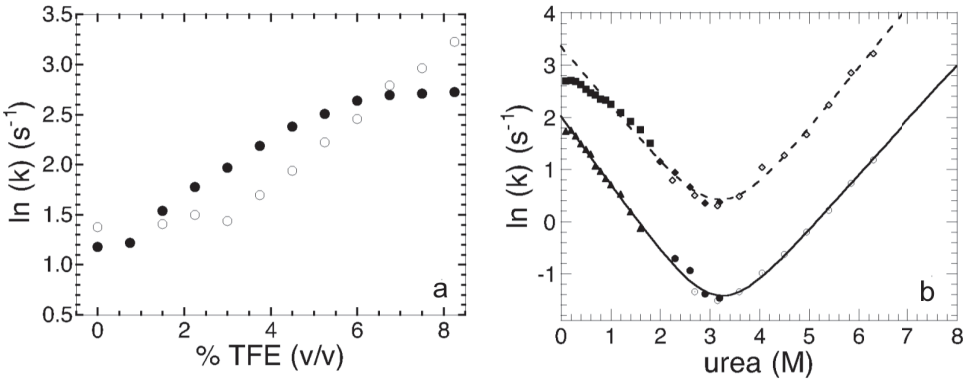

Figure 3.12 (a) Rate constants for folding in 0.6M urea (filled circles) and unfolding in 5.4M urea (empty circles) of AcPDro2 as a function of TFE concentration. (d) Rate constants for folding and unfolding of AcPDro2 as a function of urea concentration, in 0% TFE (lower trace) and 5% TFE (upper trace). Solid and empty symbols indicate folding and unfolding, respectively. Solid diamonds and solid circles indicete experiments performed by unfolding the protein in 6M urea at pH 5.5, whereas solid squares and solid triangles refer to 2M urea and pH 2.0 as initial unfolding conditions.

Both chevron plots, determined in 0 and 5% TFE, were fitted to the equation:

$$\ln k = \ln\left[k_F^{H_2O}\exp\left(m_F\left[Urea\right]\right) + k_U^{H_2O}\exp\left(m_U\left[Urea\right]\right)\right] \qquad \text{(B)}$$

edited by Jackson and Fersht (125), where $k_F^{H_2O}$ and $k_U^{H_2O}$ are the rate constants for folding and unfolding in the absence of urea, respectively and m_F and m_U are the dependencies of ln k_F and ln k_U on urea concentration, respectively. This fitting allowed us to calculate the values for the two rate constants in the absence of urea ($k_F^{H_2O}$ and $k_U^{H_2O}$, respectively). The data points between 0 and 0.6 M urea in 5% TFE were obviously excluded from the fitting procedure. $k_F^{H_2O}$ was found to be 7.5(±0.3) s^{-1} and 28.6(±2.4) s^{-1} in 0 and 5% TFE, respectively. $k_U^{H_2O}$ was found to be 4.2(±0.8)·10^{-3} s^{-1} and 1.7(±0.5)·10^{-2} s^{-1} in 0 and 5% TFE,

respectively. The $\Delta G_{U-F}^{H_2O}$ values, obtainable from equilibrium experiments, can also be obtained from kinetic data using:

$$\Delta G_{U-F}^{H_2O} = -RT\ln\left(k_U^{H_2O}/k_F^{H_2O}\right) \qquad \text{(C)}$$

where R and T are the universal gas constant and temperature, respectively. $\Delta G_{U-F}^{H_2O}$ was found to be 18.5(±0.6) kJ mol^{-1} in the absence of TFE and 18.4(±1.1) kJ mol^{-1} in 5% (v/v) TFE. These values appear to be within experimental errors to those obtained from the equilibrium chemically-induced denaturation curves (cfr with data in Fig. 3.11b). The observation that folding and unfolding are both accelerated by ca. 4 times upon the addition of small quantities of TFE provides an explanation as to why the conformational stability of AcPDro2 (i.e. $\Delta G_{U-F}^{H_2O}$) is not changed from 0 to 5% TFE.

3.5 Aggregation mechanism of AcPDro2

The results shown in the previous paragraphs show that AcPDro2 is able to form amyloid-like fibrils and protofilaments under conditions in which a native-like structure of the protein is initially populated and does not appear thermodynamically destabilised relative to the unfolded or partially folded state. One issue that is important to address is whether the fibrils (Agg) form from the partially unfolded or totally unfolded state (I) that is scarcely populated but in rapid equilibrium with the native state (N) through the folding and unfolding rate constants (Scheme 1, see below).

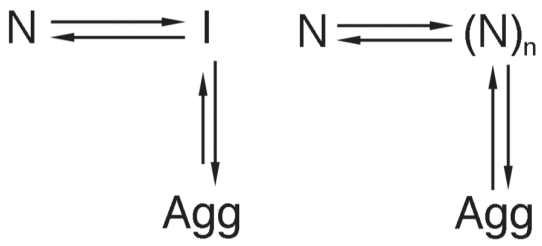

Two possible mechanisms of AcPDro2 aggregation. (left) Scheme 1: the protein may for fibrils from a totally or partially unfolded state (I) that is scarcely populated but in rapid equilibrium with the nativa state (N) through the folding and unfolding rate constants. (right) Scheme 2: various molecules of native AcPDro2 may assemble and subsequently undergo a structural reorganization to form the observed amyloid-like fibrils.

Alternatively the protein may fibrillate via a pathway in which various molecules of native AcPDro2 assemble and subsequently undergo a structural reorganisation to form the observed amyloid-like fibrils (Scheme 2, see above). If scheme 1 is correct to describe the aggregation process of AcPDro2 under the investigated conditions the apparent rate constant for aggregation (k_{obs}) results from a combination of the unfolding and folding rate constants ($k_U^{H_2O}$ and $k_F^{H_2O}$) and of the rate constant for the conversion of the partially unfolded ensemble into aggregates (k_{agg}). Kinetic inspection of the system and matrix algebra leads to (110):

$$k_{obs} = k_{agg} k_U^{H_2O} / \left(k_U^{H_2O} + k_F^{H_2O} \right) \qquad \text{(D)}$$

To determine k_{obs}, AcPDro2 was incubated at a concentration of 0.4 mg ml^{-1} in 5% TFE. The steady-state fluorescence of ThT was measured at different time points in the presence of aliquots of the protein sample that had undergone aggregation in the absence of ThT. The plot of ThT fluorescence versus time was fitted to a single exponential function to determine the k_{obs} value (Fig. 3.13), according to the equation:

$$F(t) = F_{eq} + A \exp\left(-k_{app} t \right) \qquad \text{(E)}$$

where $F(t)$ is the ThT fluorescence at time t, F_{eq} is the maximum ThT fluorescence obtained at the end of the observed exponential phase, A is the amplitude of the fluorescence change and k_{app} is the apparent rate constant.

The experiment and analysis were repeated three times and the kinetic profiles were found to be superimposable and reproducible. The fitting procedure yielded values of $2.9\pm(0.3)\cdot10^{-5}$, $2.4\pm(0.4)\cdot10^{-5}$ and $2.5\pm(0.2)\cdot10^{-5}$ s^{-1} for the k_{obs} value in the three cases.

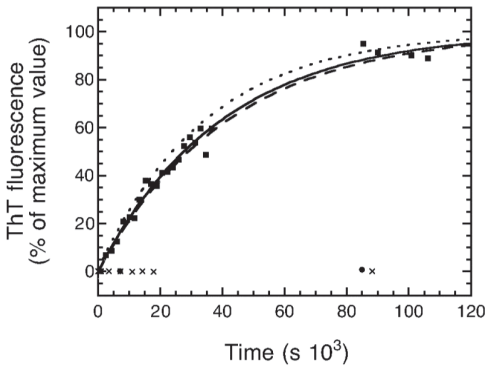

Figure 3.13 Time course of aggregation of AcPDro2 in 5% TFE. The zero time point refers to the addition of TFE to the protein solution. The experiment has been repeated three times, although only one representative set if data is shown. The solid line through the data represents the best fit of the data set shown to a single exponential function (Eq. E). The two dashed lines represent the best fit for the other two sets of data. The figure also show data for experiments in which AcPDro2 was incubated under the same conditions in absence of TFE (solid circles) and in 5% TFE at pH 3.5 (crosses).

While the $k_U^{H_2O}$ and $k_F^{H_2O}$ values have been determined under the conditions explored here $(1.7(\pm0.5)\cdot10^{-2}$ and $28.6(\pm2.4)$ s^{-1}, respectively), the k_{agg} value is difficult to determine experimentally under such conditions because the non-aggregated protein populates initially a native-like rather than unfolded or partially unfolded state. This problem was circumvented, however, with two approaches. First the k_{agg} value has been calculated using the algorithm edited by DuBay et al. (48), allowing the rate constant for aggregation to be calculated for any unstructured amino acid sequence at a desired protein concentration, pH and ionic strength. The value of k_{agg} for AcPDro2 under the conditions investigated here is predicted to be $4.5(\pm3.0)\cdot10^{-5}$. Second, the k_{agg} value has been determined under conditions in which the protein is

substantially unfolded. A pH-titration experiment showed that AcPDro2 is over 95% unfolded in 5% TFE at pH lower than 4 (data not shown). The kinetic profile of the aggregation process has therefore been followed at pH 3.5 (see *Materials and methods* for details). Aggregation was found to be very slow with no aggregates formed to any significant extent up to 24 hr (Fig. 3.13). An experimental bound can be $k_{agg} < 2 \cdot 10^{-6}$. This bound has been determined in 5% (v/v) TFE at pH 3.5 and is not, therefore, correct for the conditions of interest here (5% TFE, pH 5.5). This bound can be corrected using the previously determined relationship between k_{agg} and net charge (139), leading to an experimental bound of $<2 \cdot 10^{-5}$ s^{-1} for k_{agg} in 5% TFE, pH 5.5, with an order of magnitude similar to the predicted value.

Substitution of the experimentally determined values of $k_U^{H_2O}$ and $k_F^{H_2O}$, and of the predicted value of k_{agg} in equation (D) leads to a value of $2.65(\pm 1.95) \cdot 10^{-8}$ s^{-1} for k_{obs}, 3 orders of magnitude lower than that determined experimentally [$k_{obs}=2.6(\pm 0.3) \cdot 10^{-5}$ s^{-1}]. Using the experimental bound $<2 \cdot 10^{-5}$ s^{-1} for k_{agg}, a bound of $<1 \cdot 10^{-8}$ s^{-1} is obtained for k_{obs}, again far from that determined from the kinetic profile. This discrepancy indicates that scheme 1 is not correct and that AcPDro2 can aggregate without unfolding into a fully or partially unfolded state under these conditions.

3.6 Discussion

It is generally believed that globular proteins need to unfold, at least partially, to aggregate into amyloid or amyloid-like fibrils (21,34,75,132). Such a "conformational change hypothesis" is widely supported by a large body of

experimental data. Proteins normally adopting a compact and well defined three dimensional fold have a higher propensity to aggregate under conditions that promote their partial unfolding, such as high temperature, high pressure, low pH or moderate concentrations of organic solvents (79-81,140). In addition, for some diseases in which the aggregating proteins normally adopt folded conformations, evidence suggests that a destabilisation of the native structure, resulting in an increase in the population of non-native states, is one of the mechanisms of action through which the pathogenicity of natural mutations is mediated; this was shown for proteins such as human lysozyme, transthyretin, superoxide dismutase and the immunoglobulin light chain (73,82,131,141). Amyloid formation by proteins that have no link to human disease is also promoted by destabilising mutations both in vitro and in vivo (40,79,142).

Although the "conformational change hypothesis" is undoubtedly correct to describe the aggregation mechanism of many globular proteins, the results presented here for AcPDro2 and additional evidence reported recently for other proteins question the general applicability of this theory. Under the conditions of pH, ionic strength and temperature investigated here, AcPDro2 is stable in its native conformation in the absence of TFE, with a free energy change of unfolding ($\Delta G_{U-F}^{H_2O}$) of ca. 18 kJ mol^{-1} and no apparent aggregates formed after 24 hr. In the presence of a small concentration of TFE, such as 5% (v/v), the protein assembles into fibrillar aggregates able to bind ThT and CR and having extensive β-sheet structure. Under these conditions AcPDro2 maintains a native-like conformation prior to aggregation. Indeed, the protein has a secondary structure content, packing around aromatic and hydrophobic residues, hydrodynamic diameter and catalytic activity indistinguishable from

those of the native protein kept under conditions that do not promote aggregation. More importantly, the thermodynamic stability of the native conformation was found to be similar under native and aggregating conditions, with folding and unfolding appearing both accelerated to similar extents.

In a previous study it has been shown that the *E. coli* HypF-N aggregates under conditions in which the protein is still folded, a result that is apparently similar to that described here for AcPDro2 (110). Yet, HypF-N was found to be energetically destabilised under conditions promoting aggregation and the kinetic analysis revealed that aggregation can indeed occur from a partially folded conformation, such as that accumulating during folding, which is at equilibrium scarcely populated but still in rapid equilibrium with the native structure (110). By contrast, AcPDro2 appears to be as stable as under non-aggregating conditions and the kinetic analysis shows that the a mechanism of aggregation via partial unfolding is largely inconsistent with the experimental data. An alternative model, in which the protein is not viewed to unfold before self-assembly, needs to be invoked to outline the aggregation mechanism of AcPDro2 in these conditions. One possibility is that native-like molecules of AcPDro2 incteract through their edge β-strands.

The question naturally arises as to why AcPDro2 requires small concentrations of TFE to aggregate. In its native state human muscle acylphosphatase, a protein sharing 36% sequence identity and belonging to the same structural family as AcPDro2 (143), undergoes limited proteolysis by trypsin, chymotrypsin, elastase and subtilisin at the same sites along the sequence in the presence and absence of 10% TFE. However, the rate of proteolysis appears to be more rapid at all sites in 10% TFE, indicating that the

native protein has gained flexibility in the presence of TFE (143). It is reasonable that in the presence of small concentrations of TFE the native fold of a protein, such as AcPDro2, becomes flexible and plastic enough so that more opportunities exist for intermolecular interactions to occur within the context of native or native-like structures.

While this hypothesis is actually under investigation by performing NMR assignments on AcPDro2, incubated both in 0% and in 5% TFE, the most important message that emerges from this study is that folded proteins can aggregate into fibrillar aggregates under conditions that do not promote their unfolding or destabilisation. In the highly crowed environment of a cell, or in the extracellular space where macromolecules still overcrowd the available space, albeit to a lower extent, native proteins have to face a considerable number of events that can possibly alter and distort their fold or simply increase their flexibility. Specific interactions with ligands and partner proteins, non-specific interactions with a variety of alcohols or lipids that are present *in vivo* and translocation between organelles across phospholipid membranes are just a few examples in which this can occur. Perhaps the evolutionary adaptations that all-β proteins have designed to prevent aggregation via interactions of the edge strands of their native β-sheets is the most intriguing indication that native or native-like aggregation is indeed possible and needs to be actively combated by living organisms (144).

CHAPTER IV – RESULTS

Effects of inorganic phosphate on stability and aggregation propensity.

4.1 Introduction

In Chapter III of this thesis, we show that AcPDro2 can form, in 5% (v/v) trifluoroethanol (TFE) at pH 5.5 and 25 °C, aggregates with a morphology and diameter typical of amyloid fibrils, a high content of β-sheet structure and an ability to bind CR and ThT. Under such conditions AcPDro2 was found to have, before aggregation, a fully native structure; moreover, it was also shown to have a conformational stability, expressed as free energy change of unfolding ($\Delta G_{U-F}^{H_2O}$), apparently identical to that determined in the absence of TFE, i.e. under conditions in which the protein does not aggregate. The time-course of fibril formation was shown to be remarkably more rapid than that expected from models in which the protein is viewed to unfold before assembly, leading to the aggregation scheme reported in Figure 4.1a.

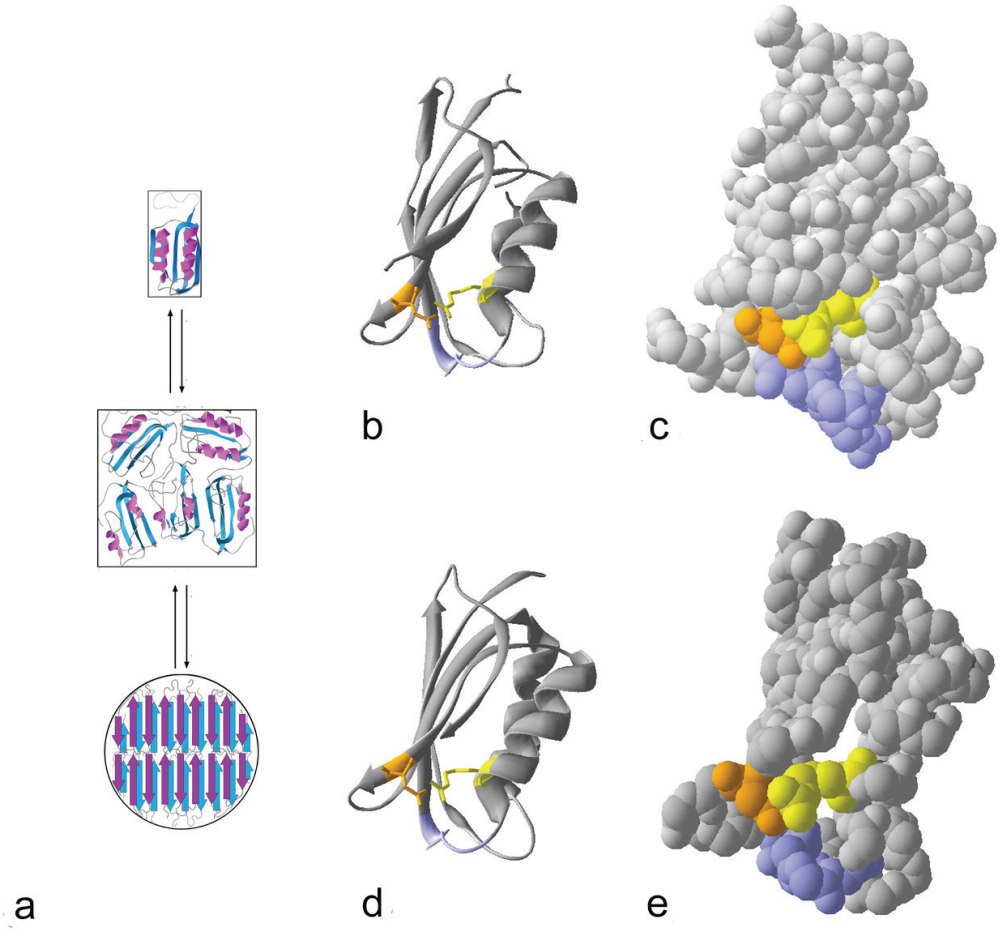

Figure 4.1 Three-dimensional structures and aggregation pathways of AcPDro2 and Sso AcP. (a) Mechanisms of aggregation of AcPDro2 into amyloid-like fibrils or Sso AcP into amyloid protofibrils, under conditions in which both proteins are initially native. Both proteins were shown to undergo assembly and, subsequently, a structural reorganisation to form amyloid-like structures. Scheme from (78). (b,c,d,e) Three-dimensional structures of native AcPDro2 (b,c) and Sso AcP (d,e) shown by secondary structure (b,d) and space-fill (c,e) representation as determined by X-ray crystallography (PDB codes are 1URR and 2BJD, respectively). In all structures, residues of the active site are shown in yellow (Arg27 and Arg30 in AcPDro2 and SsoAcP, respectively), orange (Asn45 and Asn48, respectively), and blue (residues GXVQGV at positions 19-24 and 22-27, respectively). All structures are obtained using the SwissPDBViewer software.

It is well known that a good number of proteins that can give rise to amyloid-related pathologies are normally folded, in their soluble states, into globular units with persistent secondary structure and long-range interactions; examples include β2-microglobulin, transthyretin (TTR), lysozyme, immunoglobulin light chain, superoxide dismutase-type 1 (SOD-1), insulin, cystatin c, gelsolin, lactoferrin and prolactin (17,21).

Although the so-called "conformational change hypothesis", in which is assumed that amyloid formation from an initially folded protein generally requires partial or total unfolding (4,17,21,75), is certainly appropriate to explain the aggregation behaviour of many folded proteins, evidence is mounting that proteins retain a small yet significant propensity to aggregate when folded into their native structures. Models in which partial or complete unfolding is ruled out, at least in the initial step(s) of the complex process of fibril formation, have been described for human insulin (77), Ure2p from *Saccharomyces cerevisiae* (145), the variable domain of an immunoglobulin light chain, called LEN (146), human lithostathine (147), the acylphosphatase from *Sulfolobus solfataricus* (69,78), the S6 protein from *Thermus thermophilus* (56), human ataxin-3 (133) and the isoform 2 of acylphosphatase from *Drosophila melanogaster* (112).

If a globular protein undergoes aggregation without unfolding, at least in the early steps of the process of self-assembly when the first oligomers form, the question naturally arises as to whether strategies designed to stabilise the globular native state represent an effective therapeutic means to inhibit aggregation and contrast disease onset. This is an important issue as it is increasingly recognised that the small oligomers, rather than the mature fibrils, represent the pathogenic species in many protein deposition diseases. In this work we use the acylphosphatases from *D. melanogaster* (AcPDro2) and *S. solfataricus* (Sso AcP) to explore the effect on amyloid aggregation of a ligand binding specifically to the native states of these two proteins. Unlike other acylphosphatases so far investigated, namely the N-terminal domain of E. Coli HypF (HypF-N) and human muscle acylphosphatase (35,110), AcPDro2 and Sso AcP were previously shown to aggregate, under conditions in which their

native states are initially populated, by forming assemblies in which the proteins retain a native-like structure that only later convert into amyloid-like protofibrils and/or fibrils (Fig. 4.1a) (69,78,112).

Similarly to all the acylphosphatases so far characterised, AcPDro2 and Sso AcP are α/β proteins with a ferredoxin-like fold (Fig. 4.1b,d) (91,94) and an ability to catalyse the hydrolysis of acylphosphates (91,111). From structural inspection and a detailed mutational study carried out on the homologous human muscle acylphosphatase (96-98), the active site of AcPDro2 appears to be formed by Arg27, Asn45 and the loop 20-25 (Fig. 4.1b,c). These correspond to Arg30, Asn48 and loop 23-28 for Sso AcP (Fig. 4.1d,e). The Arg residue is mainly involved in acylphosphate binding, whereas the Asn residue binds to the water molecule promoting hydrolysis and participates to catalysis (97,98). Importantly, the active site can also bind specifically, by means of the Arg residue, to a number of competitive inhibitors containing either a phosphate or sulfate group (4,95).

The kinetically well characterised pathways of amyloid aggregation for AcPDro2 and SsoAcP and the ability of their native states to bind specifically to an ion as simple as inorganic phosphate make these two proteins ideal systems to investigate whether compounds binding specifically to the native folded states of amyloidogenic proteins can be effective drugs even for cases in which unfolding may not be the primary step in amyloidogenesis.

4.2 P_i stabilises native AcPDro2 and inhibits its conversion into amyloid-like fibrils.

We first investigated whether inorganic phosphate (P_i), a competitive inhibitor of acylphosphatases binding to the active site, stabilises the native structure of AcPDro2 relative to the fully unfolded state. Figure 4.2a shows urea-induced unfolding curves acquired at equilibrium in the presence of increasing concentrations of P_i and obtained using intrinsic fluorescence as a spectroscopic probe to follow unfolding. The analysis of the curves, carried out using a two-state model (124), yielded for each of the investigated P_i concentrations, the values of unfolding midpoint (C_m), cooperativity (m value) and free energy of unfolding extrapolated in the absence of denaturant ($\Delta G_{U-F}^{H_2O}$). These are reported in Table 4.1, below.

Table 4.1 Parameters for Enzymatic Activity, Equilibrium Unfolding and Aggregation of AcPDro2 variants.

Variant	Specific activity (I.U. mg^{-1}) [a]	C_m (M)[b]	$\Delta G_{U-F}^{H_2O}$ (kJ mol^{-1})[b,c]	k_{obs} (s^{-1})[d]
wt / 0 mM P_i	1280	2.65±0.1	15.5±0.7	$1.7(\pm0.1)\cdot10^{-3}$
wt / 1 mM P_i		2.9±0.1	16.9±0.7	$1.2(\pm0.1)\cdot10^{-3}$
wt / 2 mM P_i		3.1±0.1	17.9±0.7	$6.3(\pm0.6)\cdot10^{-4}$
wt / 5 mM P_i		3.35±0.1	19.6±0.7	$1.9(\pm0.2)\cdot10^{-4}$
wt / 10 mM P_i		3.45±0.1	20.1±0.7	$9.1(\pm0.6)\cdot10^{-5}$
R27A / 0 mM P_i	Not detectable (~0)	4.3±0.1	25.1±0.8	$3.5(\pm0.5)\cdot10^{-3}$
R27A / 5 mM P_i		4.45±0.1	25.9±0.8	$4.0(\pm0.5)\cdot10^{-3}$
N45A / 0 mM P_i	Not detectable (~0)	3.3±0.1	19.4±0.7	$6.1(\pm0.3)\cdot10^{-4}$
N45A / 5 mM P_i		3.7±0.1	21.6±0.7	$2.3(\pm0.2)\cdot10^{-4}$

[a] Determined in 50 mM acetate buffer, pH 5.5, 25 °C, using 4 mM benzoylphosphate as a substrate. I.U., international units.

[b] Determined from equilibrium urea-unfolding experiments analysed according to a two-state model (124).

[c] $\Delta G_{U-F}^{H_2O}$ values were calculated using $\Delta G_{U-F}^{H_2O} = \underline{m} \cdot C_m$, where $\underline{m}$ equals 5.8±0.1 kJ mol^{-1} M^{-1} (average *m* value from all the acquired curves).

[d] Aggregation rate constants determined from time-courses of ThT fluorescence analyzed with equation E (see chapter III). Conditions were 10%, 13% and 11% (v/v) TFE for wild-type, R27A and N45A AcPDro2, respectively.

The C_m value appears to increase with P_i concentration (Fig. 4.2a and Table 4.1). Since the *m* value appears to be substantially similar under the various conditions, the $\Delta G_{U-F}^{H_2O}$ also appears to increase with P_i concentration (Table 4.1).

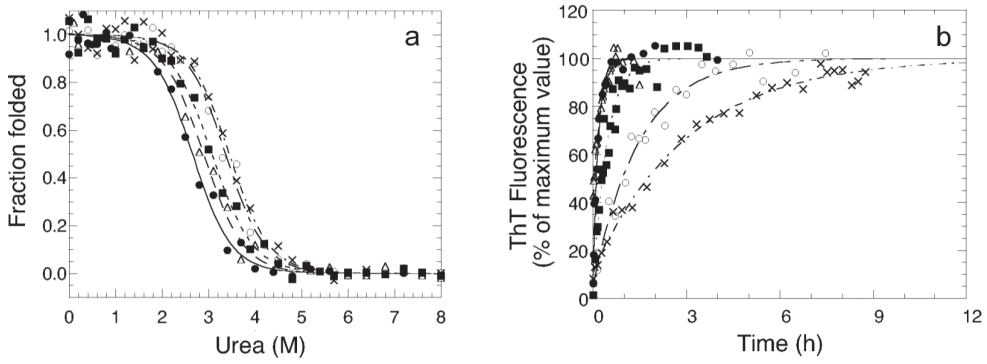

Figure 4.2 . (a) Equilibrium urea unfolding curves of wild-type AcPDro2 in 0 mM (solid circles), 1 mM (open triangles), 2 mM (solid squares), 5 mM (open circles), and 10 mM (crosses) P_i. The lines represent the best fits to the two-state equation previously described (124).(b) Time-course of aggregation of 0.4 mg ml^{-1} wild-type AcPDro2 in 10% (v/v) TFE with various amounts of P_i (symbols as in figure 15a). The zero time point refers to the addition of TFE to the protein solution. The lines through the data represent the best fits to a single exponential function (equation E, see chapter III). In both panels conditions were 50 mM acetate, 2 mM DTT, pH 5.5, 25°C.

We then studied aggregation of AcPDro2 at P_i concentrations ranging from 0 to 10 mM. Under such conditions AcPDro2 is initially native (data not shown). Aggregation of AcPDro2, followed using the ThT fluorescence assay, was found to be increasingly slower as the P_i concentration increases (Fig. 4.2b and Table 1).

4.3 P_i has no effect on an AcPDro2 mutant lacking the main residue involved in binding.

To investigate further whether the inhibitory effect of P_i on amyloid formation arises from the ability of this compound to bind to and stabilise the protein in its native conformation, or rather from another non-specific effect, two single mutants of AcPDro2 were produced, having Arg27 and Asn45 substituted with alanine, respectively (R27A and N45A AcPDro2). From a detailed study carried out on the homologous human muscle acylphosphatase (98), Arg27 is known to be main binding site of both the substrate and competitive inhibitor. Accordingly, R27A AcPDro2 appears to be enzymatically inactive (Table 4.1) and does not appear to be stabilised by the addition of 5 mM P_i (Fig. 4.3a, Table 4.1). In addition to having no stabilising effect of the native structure of AcPDro2, P_i was also found to have no detectable effect on the aggregation rate of AcPDro2, at the same concentration of 5 mM (fig. 4.3b). This allows the P_i-mediated inhibition of amyloid fibril formation to be closely linked to the ability of the compound to bind to, and stabilise, the native structure of the protein.

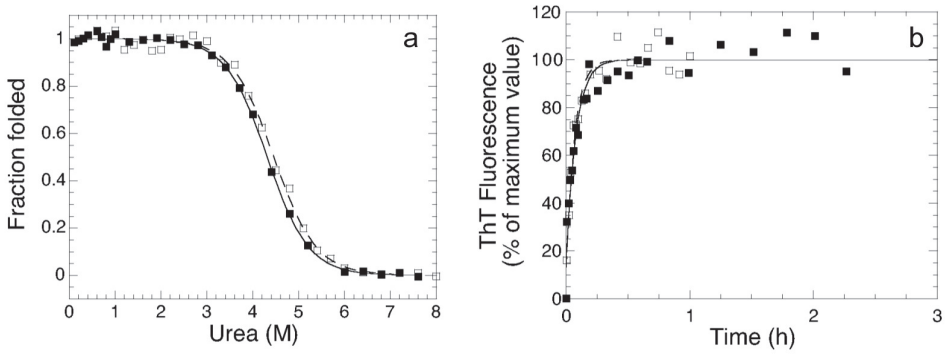

Figure 4.3 (a) Equilibrium urea unfolding curves for R27A in 0 mM (solid squares) and 5 mM (open squares) P_i, The lines represent the best fits to the two-state equation previously described (124). (b) Time-course of aggregation of 0.4 mg ml^{-1} R27A in solutions containing 0 mM and 5 mM P_i (symbols as in panel a). The zero time point refers to the addition of TFE to the protein solution. The lines through the data represent the best fits to a single exponential function (equation E). Experimental conditions were 0% (a) and 13% (b) TFE, 50 mM acetate buffer, 2 mM DTT, pH 5.5, 25 °C.

4.4 P_i inhibits amyloid formation of a catalytically inactive variant in which P_i binding is retained.

Asn45 is thought to be mainly involved in catalysis, rather than substrate and P_i binding, from the study performed on the corresponding Asn41 of human muscle acylphosphatase. (97) N45A AcPDro2 has lost its acylphosphatase activity (Table 1), but can still bind to, and be stabilised by, P_i (Table 4.1 and Fig. 4.4a). The increases of C_m and $\Delta G_{U-F}^{H_2O}$ following the addition of 5 mM P_i were 0.40 M and 2.2 kJ mol^{-1}, respectively (Table 4.1). These values were lower than those of the wild-type protein (0.7 M and 4.1 kJ mol^{-1}, respectively), indicating that although the N45A mutant retains an ability to bind to P_i, it does so with a lower binding affinity. The aggregation of N45A AcPDro2 is significantly retarded in the presence of 5 mM P_i (Fig. 4.4b), although the deceleration is only 2.6-fold and lower than that of the to wild-type protein, 8.9-fold (Table 4.1). This result can be effectively explained by considering that the native state of the

N45A mutant has a retained, but decreased, ability to bind to P_i relative to the wild-type protein.

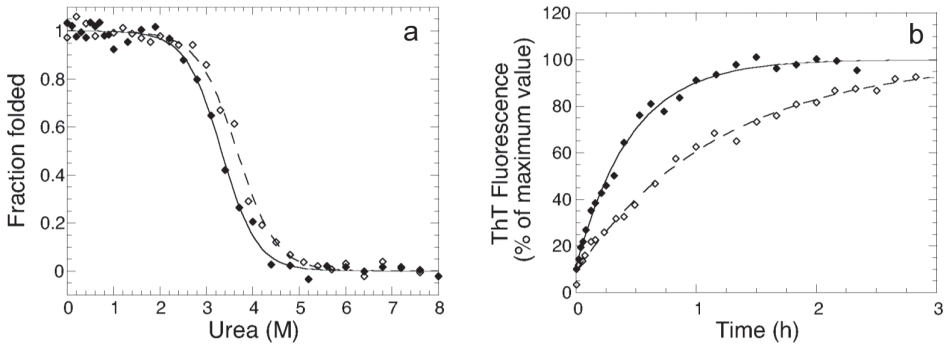

Figure 4.4 (a) Equilibrium urea unfolding curves for N45A in 0 mM (solid diamonds) and 5 mM (open diamonds) P_i. The lines represent the best fits to the two-state equation previously described (124). (b) Time-course of aggregation of 0.4 mg ml^{-1} N45A in solutions containing 0 mM and 5 mM P_i (symbols as in panel a). The zero time point refers to the addition of TFE to the protein solution. The lines through the data represent the best fits to a single exponential function (equation E). Experimental conditions were 0% (a) and 11% (b) TFE, 50 mM acetate buffer, 2 mM DTT, pH 5.5, 25 °C.

4.5 P_i slows down the formation of native-like oligomers by Sso AcP.

Sso AcP is a hyperthermophilic protein with a $\Delta G_{U-F}^{H_2O}$ of 48 kJ mol^{-1} at pH 5.5, 37 °C (106), and unfolding occurring only under very harsh conditions (91). In 15-25% (v/v) TFE, pH 5.5, 25 °C the protein populates, before aggregation initiates, a native-like conformation (69). On the time-scale of 1-2 minutes oligomers form in which the protein molecules retain a marked enzymatic activity (78). These species do not yet bind CR, ThT and ANS; nor do they show an extensive β-sheet structure, as revealed by far-ultraviolet circular dichroism (far-UV CD) and Fourier-transform infra-red spectroscopy (FTIR) (78). In spite of a native-

like topology, the secondary structure appears to be changed to some extent (78).

These oligomers further convert directly, on the time scale of several minutes with no need of dissociation and re-nucleation, into another type of aggregates which bind CR, ThT and ANS, possess extensive β-sheet structure and lack enzymatic activity (78). Using transmission electron microscopy these species appear to have a morphology typical of amyloid protofibrils, i.e. spherical aggregates with a diameter of 3-5 nm, or chain-like aggregates in which the constituent beads again have a diameter of 3-5 nm (78). Formation of the first and second types of aggregates occur 2 and 4 orders of magnitude more rapidly than unfolding of the native monomer under the same conditions, ruling out the need to unfold to initiate aggregation (Fig. 4.1a) (69). Our ability to resolve on the time-scale the formation of the native-like oligomers and their further conversion into amyloid protofibrils provides a unique opportunity to investigate the effect of P_i on the two aggregation phases separately.

Self-assembly of native monomers into native-like oligomers can be effectively followed by monitoring the change of ellipticity at 208 nm ($[\theta_{208}]$) since the difference of CD signal is maximal at this wavelength (78). Incubation of wild-type Sso AcP in 20% (v/v) TFE yields a rapid increase of $[\theta_{208}]$ followed by a much slower increase (Fig. 4.5), with these changes attributable to the first and second aggregation phases, respectively (89). The addition of 1 or 2 mM P_i causes the first rapid increase of $[\theta_{208}]$ to be slower and lower in magnitude (Fig. 4.5). This indicates that P_i slows down the formation of the native-oligomers and causes the conformational change associated with their formation to be less significant than in the absence of P_i.

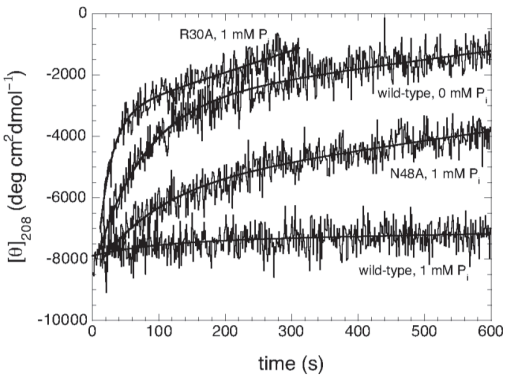

Figure 4.5 Self-assembly of native, monomeric Sso AcP into native-like oligomers followed by far-UV CD at 208 nm. The 4 traces refer to wild-type Sso AcP with and without P_i, R30A Sso AcP with P_i and N48A Sso AcP with P_i, as indicated in the graph. The solid lines through the traces represent the best fits to equation F (see below). The resulting rate constant is called k_1^{CD}. Experimental conditions were 20% (v/v) TFE, 50 mM acetate, pH 5.5, 25 °C.

P_i has no effect, and a significant decelerating effect, on this aggregation phase for the R30A and N48A mutants of Sso AcP, respectively (corresponding to the R27A and N45A variants for AcPDro2). In the presence of P_i R30A Sso AcP assembles with a rate even higher than the wild-type protein in the absence of P_i (Fig. 4.5), probably as a result of the effect of the mutation on aggregation (the mutation decreases the net charge of Sso AcP, thus facilitating aggregation relative to the wild-type). By contrast, aggregation of the N48A mutant in the presence of 1 mM P_i appears to be slower, and involve a lower amplitude change of $[\theta_{208}]$, than for the wild-type protein in the absence of the ligand (Fig. 4.5). These results allow the inhibitory effect of P_i on the formation of native-like oligomers to be coupled again to the specific binding of the ligand with the native monomeric protein.

Rate constants have been determined by fitting traces to equation:

$$[\theta]_{208}(t) = [\theta]_{208}(eq) + A\exp(-k_{obs}t) + a + bt \qquad \text{(F)}$$

where $[\theta]_{208}(t)$ is the mean residue ellipticity at 208 nm at time t, $[\theta]_{208}(eq)$ is the value obtained at the end of the observed exponential phase, A is the amplitude of the $[\theta]_{208}$ change, k_{obs} is the apparent rate constant, a and b are the coefficients

of the slower kinetic phase that on this relatively short time scale can be approximated to a straight line.

4.6 P_i also decelerates the conversion of native-like oligomers into amyloid-like protofibrils.

The second step of aggregation, that is the conversion of the native-like oligomers into the amyloid-like protofibrils, can be followed by monitoring the exponential increase of ThT fluorescence as previously reported (78,89). Such an exponential increase is protein concentration independent as it involves a structural conversion within a pre-formed aggregate rather than being rate-limited by the assembly of two or more protein molecules (78). This aggregation step appears to be decelerated markedly by 1 mM P_i for wild-type Sso AcP (Fig. 4.6). This suggests that P_i can still bind to, and stabilise, the native-like aggregates (which indeed are enzymatically active and possess the ability to bind the substrate), and disfavour their conversion into amyloid protofibrils in which the native-like topology, enzymatic activity and binding properties are lost. The same aggregation step for the R30A variant in the presence of 1 mM P_i was found to occur with a rate apparently identical to that found for the wild-type protein in the absence of P_i (Fig. 4.6), lending further support to the importance of binding specificity. Accordingly, the native-like aggregates of N45A Sso AcP, in which the substituted residue is involved in catalysis but not substrate binding, convert more slowly in the presence of P_i relative to the wild-type protein in its absence (Fig. 4.6).

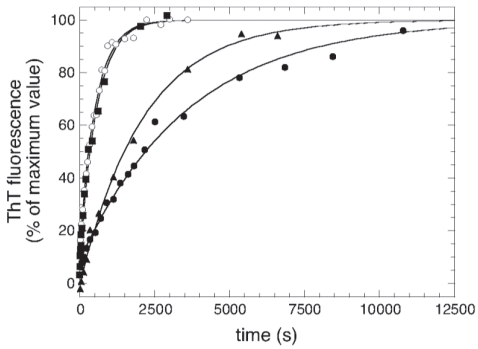

Figure 4.6 Conversion of native-like oligomers of Sso AcP into amyloid protofibrils followed by ThT fluorescence. The traces refer to wild-type Sso AcP without (open circles) and with (filled circles) 1 mM P_i, R30A Sso AcP with 1 mM P_i (filled squares) and N45A Sso AcP with 1 mM P_i (filled triangles).The solid lines through the data points represent the best fits to exponential functions (equation E). Experimental conditions were as in fig. 18.

4.7 Discussion

Several works have demonstrated that that the binding of a ligand to the native state of a folded protein is an effective therapeutic strategy to inhibit amyloid formation, when this process requires at least partial unfolding or disruption of the native quaternary structure (84-88). The results presented here suggest that the ligand-mediated stabilisation of the native state is also an effective strategy to inhibit amyloid formation even when the process does not require unfolding as an early step to trigger the process of assembly. Both the globular proteins used here aggregate more slowly in the presence of a ligand that acts physiologically as a competitive inhibitor and hence binds specifically to the active site of the native state. In both proteins the inhibitory effect is no longer present when the main substrate and inhibitor binding residue is substituted (Arg27 and Arg30 for AcPDro2 and Sso AcP, respectively), whereas it is maintained when the main catalytic site, that is not involved in binding, is replaced (Asn45 and Asn48 for AcPDro2 and Sso AcP, respectively). Although the two proteins used here are not involved in any protein deposition disease

and P_i binds to them with an affinity that could not be exploitable in pharmacological research, these results underlie the concept that stabilisation of the native conformation of amyloidogenic proteins by specific binding can represent a strategy of general interest for inhibiting aggregation and amyloid formation *in vivo*.

In the aggregation process of Sso AcP, where the formation of the native-like oligomers can be studied independently of their later conversion into amyloid-like protofibrils, the ligand appears to retard both aggregation phases. These findings indicate that following binding with the ligand both the monomeric native state and the early oligomeric native-like species are stabilised, whereas the transition state for their interconversione is affected to a lower extent or is not affected at all (Fig. 4.7).

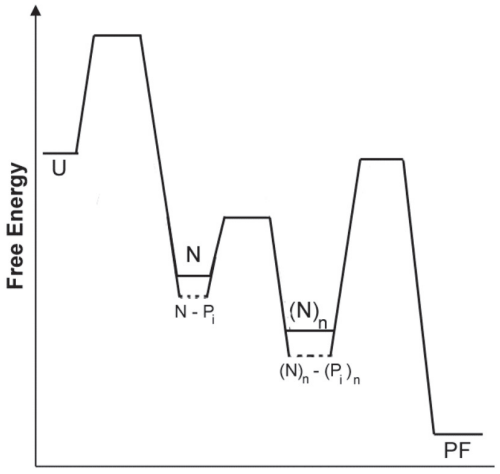

Figure 4.7 The effect of P_i on the aggregation process of Sso AcP. P_i binds to the monomeric native conformation N and the early oligomers in which the protein molecules retain a native-like conformation, $(N)_n$. Their absolute free energies decrease upon binding (dashed lines). The unfolded state U and the amyloid-like protofibrils PF do not bind to P_i and their free energies remain unaffected in the presence of the ligand. P_i may also bind to one or all the transition states reported in the scheme, but with lower affinity as their energies are found to decrease to a little, if any, extent. As a result of these effects, P_i slows down the formation of both $(N)_n$ and PF.

Similarly, the transition state for the conversion of the initial oligomers into the protofibrils is stabilised only marginally relative to the native-like oligomers. The amyloid protofibrils, in which the individual protein molecules

have undergone a major conformational change, have presumably lost completely their affinity for the ligand and therefore are not stabilised upon ligand addition. In this scenario, the free energy barriers for both aggregation phases increase in the presence of ligand, explaining the deceleration of both aggregation phases following the addition of P_i.

These results are in agreement with previously reported findings showing that destabilised mutants of SsoAcP form the early native-like oligomers and undergo the further conversion into amyloid protofibrils more rapidly than the wild-type protein (89). Although in the initial oligomers the individual protein molecules have maintained a native-like topology and enzymatic activity, far-UV CD and FTIR indicate that the protein has undergone a small but significant structural change after the transition (78). Such an aggregation event is therefore promoted by structural fluctuations, but not unfolding, that are facilitated by destabilising mutations, but are certainly disfavoured by the "freezing" of the native structure in the protein-ligand complex. The rate of the second phase of aggregation also increases with destabilsing mutations and decreases following the addition of the ligand. In this case a substantial and global structural conversion has to occur from the native-like molecules into an amyloid protofibrillar state in which there is apparently no detectable sign of native-like structural elements.

CHAPTER V – RESULTS

Effect of introducing protective structural features on stability and aggregation pathway.

5.1 Introduction

Considering that the majority of protein molecules spend most of their lifetime in a folded state, it's very important to focus efforts on elucidation of the mechanisms of aggregation from native or native-like conformations. Literature reports a lot of cases in which both pathogenic and non-pathogenic proteins can aggregate and give amyloid deposition starting from native or native-like state, such as human β-2 microglobulin (148), hen lysozyme (149), AcPDro2 (112), lithostatin (147), the S6 protein from T. Thermophilus (56) and the yeast Ure2p prion (145). Interestingly, the yeast Hsp40 chaperone Ydj1 was found to inhibit fibril formation by Ure2p by binding preferentially to the globular domain of the native protein, suggesting that folded proteins or domains are species to be targeted by molecular chaperones *in vivo* to prevent their effective aggregation (150). Perhaps the most compelling evidence that "native" aggregation processes represent a real possibility for globular proteins and a constant challenge for living organisms is shown by the finding that natural all-β

proteins have developed strategies during evolution to prevent their assembly through a direct interaction of folded units (144). While newly designed all-β sheet structures are intrinsically prone to aggregation and show a great difficulty in remaining soluble even fresh-produced, natural all-β proteins can remain monomeric, soluble and fully functional for very long periods. This important characteristic is probably due to the presence of particular structural features that protect exposed β-strands of monomers from direct interactions that can lead to edge-to-edge aggregation. The previously cited work by Richardson & Richardson summarize the most relevant of these protections, among which we can find a β-helix tertiary structure with edge covering by loop and/or an α-helix (Fig. 5.1a); the classical β-propeller (Fig. 5.1b) and β-barrel structures, that pack each of the potentially aggregation-prone edges together with others in the native structure, leaving no exposed edges outward; in case of single β-sheets, the dominant strategies are the presence of proline residues and/or β-bulges in sensitive regions, or charged side chains in the central portion of the sheet (Fig. 5.1 c).

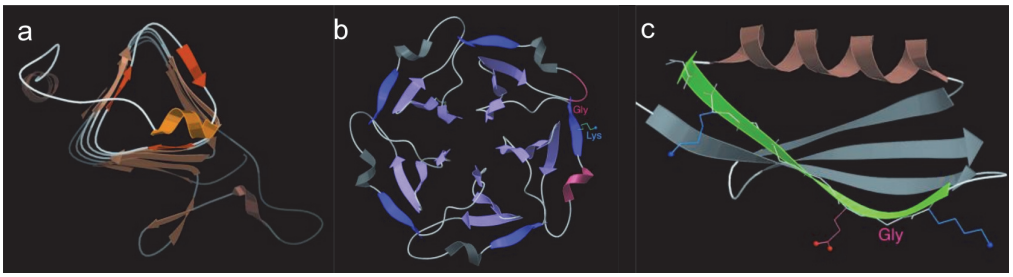

Figure 5.1 (reproduced from (144)) (a) End view of the left-handed, three-sheet β-helix of the 1QRE archaeal carbonic anhydrase. β strands are peach-colored arrows, with the three edge strands emphasized in darker orange. As is true for almost all β-helix ends, those edge strands are covered by a substantial loop, in this case containing an α-helix (in gold). (b) View down the approximate 5-fold axis of the β-propeller five structure of the 1TL2 tachylectin. β strands are lilac arrows, with edge strands of the five propeller ''blades'' in darker purple. For the edge strand on the right, the features preventing further β-sheet interactions are shown: a charged Lys, a Gly β bulge at the end of the strand, a nearby partially covering loop (pink), and a

colinear helix (pink) that blocks the first β residue. (c) A β-sheet edge strand (green arrow) that uses an Lβ Gly (labeled) to produce a large bend and a negative backbone twist for that end of the strand. The β H-bonding of that strand is completely regular, but the ''pleat'' is convex outward for three residues in a row (Lys, Gly, Gln). From the 1IGD single-sheet structure of an IGG-binding domain of Streptococcal protein G.

Finally, one of the most frequent tertiary stucture that possess these "sticky edges" is the β-sandwich, in which there are two sheets, often in anti-parallel conformation, that can potentially pack with other β-sandwich monomers, having side-by-side pairs of edge β-strands exposed (Fig. 5.2, from (144)). The main blocking strategy adopted by nature to avoid this packing is an inward-pointing charged side chain, located on the otherwise-hydrophobic β-strand that faces the opposite β-sheet (144).

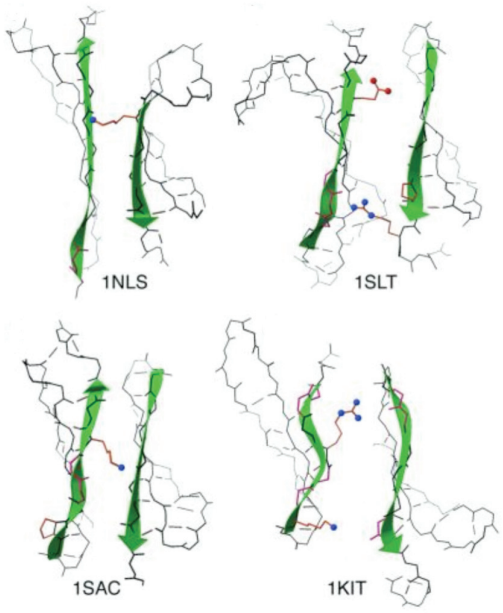

Figure 5.2 (reproduced from (144)) A set of equivalent, paired sheet edges from four different β-sandwich protein families having the lectin/glucanase fold. Edge β strands are shown as sea green arrows, β bulges in hot pink, and inward-pointing charged side chains with red or blue balls for their O or N atoms. All examples have at least one bulge and at least one inward-pointing charge, although the positioning and the overall shapes vary. From PDB files 1NLS, 1SLT, 1SAC, and 1KIT.

As detailed in Chapter III and in the introduction to Chapter IV, it was previously shown that two proteins from the acylphosphatase-like structural family, namely the acylphosphatase from *S. solfataricus* (Sso AcP) and the second acylphosphatase from *D. melanogaster* (AcPDro2) have the ability to aggregate via the transient formation of oligomers in which the protein molecules retain native-like conformations (78,112). By contrast, two other proteins from the same structural family, human muscle

acylphosphatase (mAcP) and the N-terminal domain of HypF from *E. coli* (HypF-N), have been shown to require unfolding to aggregate (79,110). In particular, aggregation of HypF-N was shown to occur, even under conditions in which the native structure is the most populated species (>98%), through the self-assembly of partially folded molecules that form after the major free energy barrier of unfolding and that are in rapid equilibrium with the native state (110). The observation of such differences in aggregation pathways within the same structural family provides a unique opportunity to explore the determinants of either mechanism. To this purpose we have compared the sequences and structures of these four proteins. On the basis of the differences resulting from this comparative inspection, we have designed mutants of Sso AcP that are able to prevent the aggregation pathway involving the formation of native-like aggregates.

5.2 A structural comparison between mAcP, HypF-N, Sso AcP and AcPDro2.

The native structures of the four proteins considered in this section of the study have all been solved with X-ray crystallography, facilitating the search of possible structural differences that can explain the different aggregation pathways of these four proteins (91,93,94,99). Table 5.1 shows that in the two proteins that need to unfold prior to aggregation (mAcP and HypF-N), the number of residues forming loops or adopting an unfolded conformation is lower than in the two proteins aggregating via the assembly of native-like

structures (Sso AcP and AcPDro2). Deletion of the unstructured 11 residues at the N-terminus of Sso AcP yields a mutant (ΔN11 Sso AcP) that does no longer form native-like aggregates (89). This indicates that the extent of unfolded regions in the native state is an important determinant of the aggregation pathway and may suggest that self-assembly of folded protein molecules is facilitated by the interaction of unstructured portions, such as loops or unstructured C- and N-terminal tails.

Table 5.1 Structural comparison between proteins from the acylphosphatase-like structural family.

Variant	N° of residues with unordered secondary structure [a]	N° of protective features at the edge β strands [b]	$\Delta G_{F-U}^{H_2O}$ (kJ mol^{-1}) [c]	Surface hydrophobi-city (kcal mol^{-1}) [d]	N° of underwrapped hydrogen bonds [e]
AcPDro2	40 (39.2%)	1-2, 1	-15.5±0.7	25.7	5
Sso AcP	39 (38.6%)	1, 1	-48.7±0.7	21.5	2
HypF-N	34 (37.4%)	3, 2	-29±3	19.0	0
mAcP	32 (32.7%)	3, 3	-21.3±2.3	28.3	9

[a] Calculated using MolMol. The numbers indicate residues that do not form α-helical or β-sheet structure, that is residues adopting an unfolded conformation or forming loops.

[b] Number of structural features able to protect edge β strands from edge-to-edge aggregation, defined as described previously (144). The table indicates, for each protein, the number of such features for both β-strand 4 and β-strand 5 (before and after the comma, respectively).

[c] obtained in 50 mM acetate buffer, pH 5.5, at T= 25°C for AcPDro2, and at T=28°C for Sso AcP, HypF-N and mAcP.

[d] calculated as the sum of the hydrophobicity values of all the amino acid residues of the protein, each weighted by the % of solvent-exposure (calculated using Swiss-PdbViewer and the hydrophobicity scale of the 20 amino acids reported by Chiti et al. (47).

[e] Number of backbone hydrogen bonds having three or fewer hydrophobic residues in close proximity. An hydrophobic residue is considered in close proximity if its β-carbon is contained

within the space created by two spheres with 5 Å radii, centered on the α-carbons of the two residues forming the hydrogen bond. The ordering of proteins does not change if considering four (or less) and five (or less) hydrophobic residues. This counting has been made as described previously (45).

Nevertheless, further inspection of the four proteins indicates other important differences. It has been demonstrated that the incorporation of one of the previously described protective structural features (inward pointing charges) on the edge β-strands of newly designed β-proteins can be an effective strategy to prevent aggregation of these proteins (44). All four proteins analyzed here have one β-sheet in their folded conformation, with strands 4 and 5 representing the edge β-strands in all cases. mAcP and HypF-N, the two proteins that need to unfold prior to aggregation, have 2-3 protections on both edge β-strands (Table 5.1). By contrast, AcPDro2 and Sso AcP, the two proteins aggregating via the assembly of native structures, have only 1-2 protective features (Table 5.1). A detailed description of the protective features existing for each of the strands in all four proteins is presented in Table 5.2.

No other obvious differences were found between the four proteins that might explain their different aggregation behaviors. AcPDro2 and Sso AcP, the two proteins aggregating via the formation of native-like aggregates, have the lowest and highest conformational stabilities, respectively (Table 5.1). This rules out the importance of the native state stability in determining differences in the aggregation processes of the four proteins. Nor do the four proteins exhibit a clear trend for their content of solvent-exposed hydrophobic residues, with AcPDro2 and Sso AcP having intermediate values of superficial hydrophobicity, compared with the other two cases (Table 5.1).

Table 5.2 List of protective features existing on edge β-strands of some AcPs

Analysis of protective features at the edge β-strands mAcP, HypF-N, AcPDro2 and Sso AcP [a]

protein	Continuous H-bonding	Covering loop	β-bulges	Prolines	Inward pointing charge	Sheet edge rolls in	Very short	Very twisted β-strand	LβGly bend, reverse twist	Switch between sheets	Number of protections [b]
mAcP	none	none	75-76, 82-83	none	Glu83	none	no	none	none	none	3
	none	none	none	none	Arg23, Glu27	none	yes	none	none	none	3
HypF-N	none	none	71-72	Pro78	Arg76	none	no	none	none	none	3
	none	none	N none o	none	Glu87	none	yes	none	none	none	2
AcPDro2	none	none	75-76?, 82-83	none	No	none	no	none	none	none	1-2
	none	none	No	none	No	none	yes	none	none	none	1
Sso AcP	none	none	81-82	none	No	none	no	none	none	none	1
	none	none	none	none	No	none	yes	none	none	none	1

[a] The Table describes the protective features present for each of the four proteins analysed in this work for the two edge β-strands. Each cell reports the results of the first edge β-strand (upper line) and second edge β-strand (lower line).

[b] total number of protective features given by the sum of protections described in the previous columns.

The four proteins were also compared for their number of underwrapped hydrogen bonds (UWHBs) – that is backbone hydrogen bonds surrounded by three or fewer hydrophobic residues and thus vulnerable to water attack. A high number and a high local density of UWHBs have been proposed to increase dramatically the aggregation propensity of a folded protein and even to be a distinctive feature of folded proteins associated with pathological amyloid aggregation (45). However, AcPDro2 and Sso AcP do not clearly exhibit more UWHBs than the other two proteins (Table 5.1).

From this structural comparison it appears that the lower number of protections on the edge β-strands of native Sso AcP and AcPDro2 could be a reason why such proteins can form native-like aggregates as a first step of the process of amyloid formation. Sso AcP has been studied in deeper detail than AcPDro2. Moreover, the formation of the native-like aggregates is faster than the subsequent reorganization into amyloid protofibrils, allowing accumulation and direct monitoring of native-like assemblies. β-strand 4, as opposed to the other edge β-strand 5, has been shown to play a key role in the first phase of the aggregation process of this protein (89). For these reasons we have chosen to focus our attention on the edge β-strand 4 of Sso AcP. Three mutants were produced and purified. Figure 5.3 shows the X-ray structure of Sso AcP along with the positions of the mutated residues, whereas Table 5.3 lists the mutants produced.

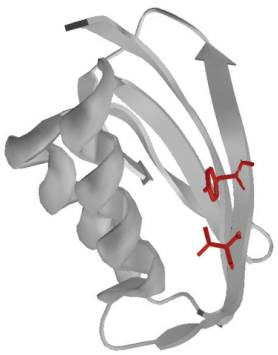

Figure 5.3 Three-dimensional structure of native Sso AcP as determined by X-ray crystallography (PDB code: 2BJD). Side chains of the residues mutated here (Val84 and Tyr86) are highlighted in red. The structure has been obtained using the Swiss-PDBViewer software.

Table 5.3. Parameters of Sso AcP variants in the absence of TFE

Variant	Apparent hydrodynamic diameter (nm)[a]	Specific activity (IU mg^{-1}) [b]	C_m (M) [c]	$\Delta G_{F-U}^{H_2O}$ (kJ mol^{-1}) [c]	$k_{F-U}^{H_2O}$ (s^{-1}) [d]	$k_{I-F}^{H_2O}$ (s^{-1}) [d]	$\Delta G_{F-I}^{H_2O}$ (kJ mol^{-1}) [e]
Wild-type	4.58±0.09	893±89	4.23±0.2	-46.9±2.2	2.3(±0.2) ·10^{-5}	4.6±0.5	-31.5±4.4
V84P	4.49±0.03	208±21	2.52±0.2	-28.0±2.2	2.3(±0.2) ·10^{-2}	4.6±0.5	-13.6±1.9
V84D	4.49±0.03	495±50	2.53±0.2	-28.1±2.2	2.2(±0.2) ·10^{-2}	4.3±0.5	-13.6±1.9
Y86E	4.46±0.10	306±31	3.43±0.2	-38.1±2.2	2.8(±0.3) ·10^{-4}	4.8±0.5	-25.1±3.5

[a] calculated in 50 mM acetate buffer, pH 5.5, 25 °C using DLS
[b] calculated in 50 mM acetate buffer, pH 5.5, 25 °C using 4 mM benzoylphosphate as a substrate.
[c] data obtained by GdnHCl unfolding curves at equilibrium, in 50 mM acetate buffer, pH 5.5, 37 °C.
[d] data obtained by a stopped-flow device in 50 mM acetate buffer, pH 5.5, 37 °C, in 0 M GdnHCl.
[e] calculated from $k_{F-U}^{H_2O}$ and $k_{I-F}^{H_2O}$ values using equation C (see Chapter III).

The V84D and Y86E mutations generate an additional negative charge between β-strand 4 and α-helix 2 (inward pointing charge), whereas the V84P variant creates a distortion in the β-strand conformation. Both features have been proposed to inhibit self-assembly of folded proteins via edge-to-edge interactions (144). The former has also been shown to inhibit aggregation of newly designed β-sheet proteins that would otherwise fail to remain soluble (44).

5.3 Analysis of the structure, stability and (un)folding rate of the Sso AcP mutants

The three variants have far-UV circular dichroism (far-UV CD) spectra indistinguishable from that of the wild-type protein, indicating that the mutants maintain a topology and secondary structure content similar to those of the wild-type protein (Fig. 5.4a). The apparent hydrodynamic diameters of the mutants, as determined with dynamic light scattering (DLS), are within experimental error to that of the wild-type protein, suggesting that the mutations do not induce changes in the size and compaction of the native structure (Fig. 5.4b, Table 5.3).

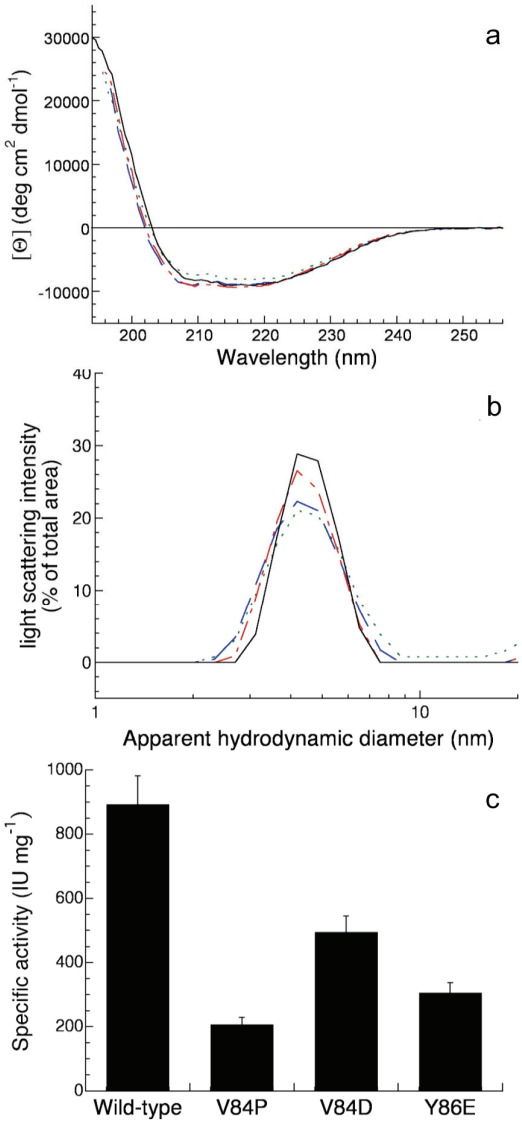

Figure 5.4 Analysis of the native states of Sso AcP variants. (a) Far-UV CD spectra for wild-type (black solid line), V84P (blue dashed line), V84D (green dotted line) and Y86E (red dashed/dotted line) Sso AcP. Spectra were recorded in 10 mM Tris/HCl, pH 8.0, 25 °C. (b) Size distribution of all variants (color code as in figure *2a*), measured by DLS in 50 mM acetate buffer, pH 5.5, 25 °C. (c) Enzymatic activity of Sso AcP mutants, measured in 50 mM acetate buffer, pH 5.5, 25 °C using 4 mM benzoylphosphate as a substrate.

All variants have enzymatic activity, providing further indication on the persistence of a native topology upon mutation (Fig. 5.4c). Interestingly, all three variants have significantly lower specific activity, compared to the wild-type protein, suggesting that the mutations introduce subtle distortions at the site of mutations that are propagated up to the active site of the enzyme. This phenomenon has also been observed for mutations of mAcP that were not in close proximity to the active site (151).

The conformational stabilities of the three variants have been investigated by means of equilibrium unfolding curves induced by guanidine hydrochloride (GdnHCl) (Fig. 5.5a). All variants appear to be destabilised, relative to the wild-type (Fig. 5.5a). In spite of the observed destabilization all variants appear to be folded in the absence of GdnHCl (Fig. 5.5a). Analysis of the equilibrium curves with a two-state model (124) allows the values of free energy change of folding in the absence of denaturant ($\Delta G_{F-U}^{H_2O}$) and the GdnHCl concentration at which 50% of the protein is unfolded (C_m) to be determined for all variants (Table 5.3).

As previously reported, the olding process of wild-type Sso AcP is complex with three kinetic phases detected during folding at low GdnHCl concentration and one phase observed for unfolding at high GdnHCl concentration, respectively (106). Figure 5.5b reports the dependence of the rate constant for unfolding (k_{F-U}, filled symbols) and of the rate constant for the conversion of the partially folded state into the fully native state (k_{I-F}, empty symbols) on GdnHCl concentration for all variants. The Y86E variant appears to have ln(k_{F-U}) values one order of magnitude higher than the wild-type protein,

when these are compared at the same denaturant concentration; the V84D and V84P variants unfold even more rapidly, three orders of magnitude faster than the wild-type (Fig. 5.5b). The dependence of $\ln(k_{F-U})$ on GdnHCl concentration appears to be linear and similar in the four proteins (Fig. 5.5b). For each variant, the linear extrapolation of the $\ln(k_{F-U})$ data to 0 M GdnHCl yields the $\ln(k_{F-U})$ value in the absence of GdnHCl (Table 5.3). The $\ln(k_{I-F})$ values of all three mutants are similar to those of the wild-type protein (Fig. 5.5b, empty symbols). The dependence of $\ln(k_{I-F})$ on GdnHCl concentration is not linear in this case and a polynomial function was used to extrapolate the $\ln(k_{I-F})$ values in 0 M GdnHCl (Table 5.3).

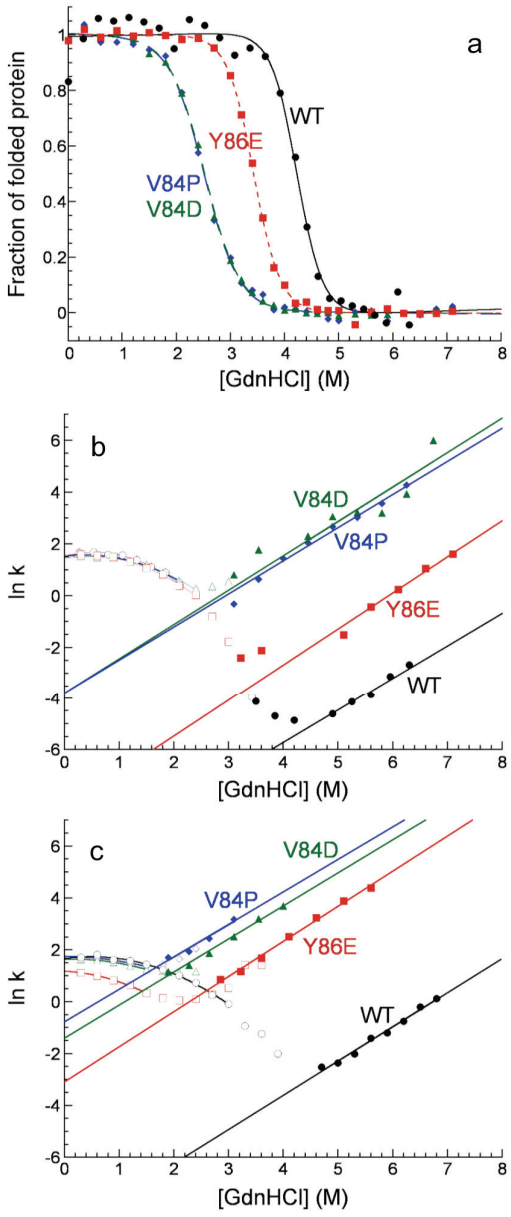

Figure 5.5 Analysis of the conformational stability, folding and unfolding rates of Sso AcP variants. (a) Equilibrium GdnHCl unfolding curves in 50 mM acetate buffer, pH 5.5, 37 °C, for wild-type (black circles), V84P (blue diamonds), V84D (green triangles) and Y86E (red squares) Sso AcP. Lines represent the best fits to the two-state equation (124). (b,c) Rate constants for folding from the partially folded state (open symbols) and unfolding (filled symbols) as a function of GdnHCl concentration, determined in 50 mM acetate buffer, pH 5.5, 37 °C, for wild-type (black circles), V84P (blue diamonds), V84D (green triangles) and Y86E (red squares) Sso AcP. The curves were obtained in the absence (b) or in the presence of 3% TFE (c) with the exception of Y86E for which 10% TFE was used (c). In all cases folding and unfolding data have been fitted to a 2nd order polynomial and a linear function, respectively (solid lines), to obtain folding and unfolding rates in the absence of GdnHCl.

Following measurements of k_{I-F} and k_{F-U} values in the absence of GdnHCl, use of well established thermodynamic laws (Equation C, see Chapter III) enables the determination, for each variant, of the free energy change resulting from the conversion of the partially folded state into the native structure, $\Delta G_{F-I}^{H_2O}$ (Table 5.3)

As described above, the three mutated forms of Sso AcP are destabilised relative to the wild-type counterpart (Fig. 5.5a, Table 5.3). Under the destabilising conditions that promote aggregation of wild-type Sso AcP - typically 20% (v/v) trifluoroethanol (TFE) - the three mutants are either unfolded or heavily destabilised (data not shown). For this reason, the aggregation processes of the mutants were compared in the presence of different TFE concentrations: 20% (v/v) TFE for wild-type, 10% (v/v) TFE for Y86E and 3% (v/v) TFE for V84D and V84D. The k_{I-F}, k_{F-U} and $\Delta G_{F-I}^{H_2O}$ values were re-determined for all the three mutants under the new conditions using the stopped-flow apparatus (Fig. 5.5c). All the re-determined values are reported in Table 5.4, which also reports the same values for the wild-type protein determined in both 3% and 20% (v/v) TFE. Under their respective conditions of TFE concentration all variants are folded prior to aggregation ($k_{I-F} >> k_{F-U}$ and $\Delta G_{F-I}^{H_2O} << 0$ in 0 M GdnHCl). This provides an opportunity to assess whether the three mutations protect Sso AcP against the formation of native-like assemblies.

Table 5.4 Parameters of Sso AcP variants in the presence of the indicated TFE concentrations

Variant	$k_{F-U}^{H_2O}$ (s^{-1}) [a]	$k_{I-F}^{H_2O}$ (s^{-1}) [a]	$\Delta G_{F-I}^{H_2O}$ (kJ mol^{-1}) [b]	k_2^{ThT} (s^{-1})
Wild-type (20% TFE)	$4.1(\pm0.4)\cdot10^{-5}$	$7.4(\pm0.7)\cdot10^{-2}$	-19.3±2.7	$3.7(\pm0.4)\cdot 10^{-3}$
Wild-type (3% TFE)	$1.4(\pm0.1)\cdot10^{-4}$	5.3±0.6	-27.1±3.8	n.d.
V84P (3% TFE)	$4.6(\pm0.5)\cdot10^{-1}$	5.7±0.5	-6.5±0.9	$6.1(\pm0.6)\cdot 10^{-4}$
V84D (3% TFE)	$2.5(\pm0.3)\cdot10^{-1}$	5.1±0.5	-7.8±1.1	$8.5(\pm0.8)\cdot10^{-4}$
Y86E (10% TFE)	$4.5(\pm0.5)\cdot10^{-2}$	3.3±0.3	-11.0±1.6	$6.0(\pm0.6)\cdot10^{-4}$

[a] data obtained in 50 mM acetate buffer, pH 5.5, 37 °C, in the absence of GdnHCl and in the presence of the TFE concentrations reported by each variant. The data for the wild-type in 20% TFE were reported previously (69).

[b] calculated from $k_{F-U}^{H_2O}$ and $k_{I-F}^{H_2O}$ values using equation C.

5.4 Analysis of the aggregation properties of the Sso AcP mutants

The first phase of Sso AcP aggregation – the aggregation of the native state into native-like, enzymatically active assemblies – is very rapid and is detectable as a rapid change of the far-UV CD spectrum (78). Figure 5.6a compares the CD spectrum of native wild-type Sso AcP, recorded in the absence of TFE, and that recorded immediately after incubation in 20% (v/v) TFE. Such a change in the CD spectrum is not observed for any of the mutants, following the addition of TFE (Fig. 5.6b-d).

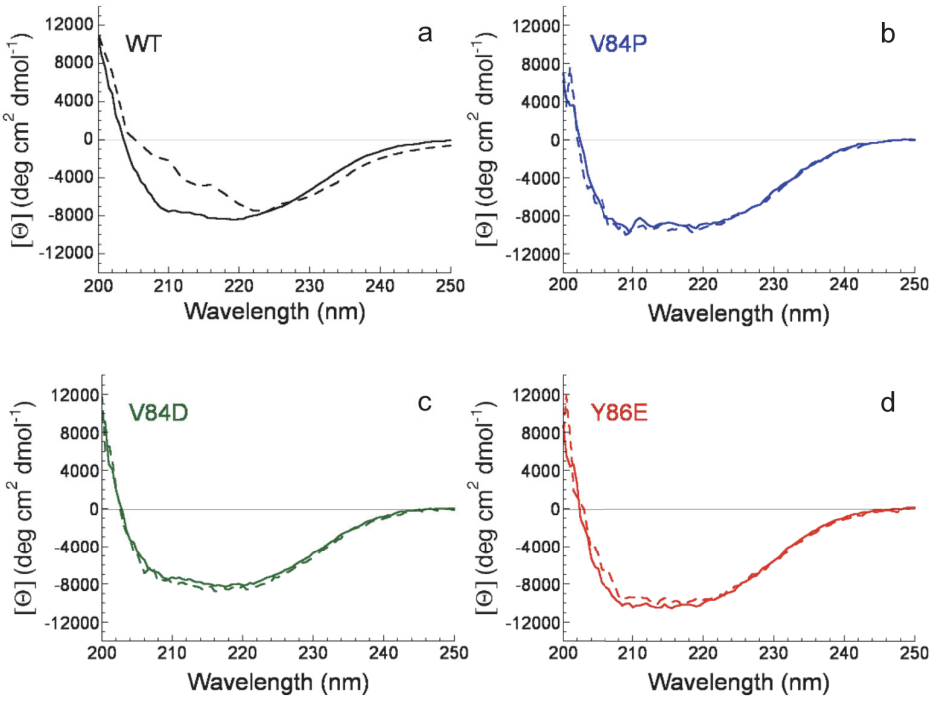

Figure 5.6 Secondary structure of Sso AcP variants under conditions promoting aggregation. (a-d) Far-UV CD spectra obtained for all variants under conditions in which the native state is stable, i.e. in 10 mM Tris/HCl, pH 8.0, 25 °C (continuous lines) and immediately after incubation in conditions promoting aggregation, that is 0.4 mg ml^{-1} protein, 50 mM acetate buffer, pH 5.5, 3-20% (v/v) TFE, 25 °C (dashed lines). TFE concentration was 20% for wild type (a), 3% for V84P (b) and V84D (c), and 10% for Y86E (d).

The maximum difference of mean residue ellipticity between the native protein and the native-like assemblies appears to occur at 208 nm (Fig. 5.6a). The time course of mean residue ellipticity at this wavelength produces a rapid, well-defined kinetic profile for wild-type Sso AcP in 20% TFE, whereas the CD signal does not appear to change for the mutants on the same time-scale (Fig. 5.7a). The first phase of Sso AcP aggregation can also be monitored with light scattering (78). Similarly to the results obtained with far-UV CD, a rapid increase of light scattering intensity is observed only for the wild-type protein (Fig. 5.7b).

The second phase of Sso AcP aggregation – the conversion of the native-like oligomers into amyloid-like protofibrils - can be monitored effectively with ThT fluorescence as the protofibrils, unlike the native-like oligomers, bind to ThT (78,89). Incubation of wild-type and three mutant Sso AcP in the presence of TFE concentrations yields an increase of ThT fluorescence in all cases, with the wild-type protein exhibiting the most rapid increase (Fig. 5.7c).

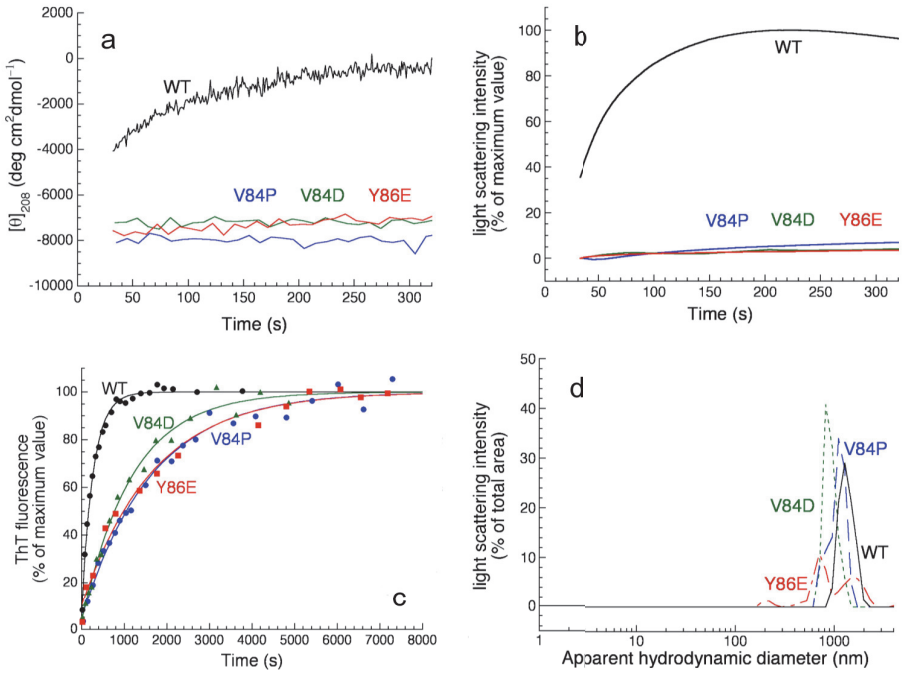

Figure 5.7 Aggregation of Sso AcP variants. (a,b) First aggregation phase (assembly of the native state into native-like aggregates) for wild-type (black), V84P (blue), V84D (green) and Y86E (red) Sso AcP, monitored by mean residue ellipticity at 208 nm (a) and light scattering intensity (b). (c) Second aggregation phase (conversion of native-like aggregates into amyloid-like protofibrils) for Sso AcP variants (color code as in panel a) monitored by ThT fluorescence. (d) Size distribution of all variants (color code as in panel a), measured by DLS after ThT fluorescence plateau has been reached. In all four panels conditions were 0.4 mg ml^{-1} protein, 50 mM acetate buffer, pH 5.5, 25 °C, in the presence of 3% TFE (V84P and V84D), 10% TFE (Y86E) and 20% TFE (wild-type).

To assess further that all mutants form aggregates and to exclude that the increase of ThT fluorescence arises from a potential binding of ThT with

partially unfolded states of the mutants we have analyzed all samples with DLS, after the ThT fluorescence had reached an apparent plateau. The size distributions of all samples clearly show the presence of aggregates (Fig. 5.7d). Since the intensity of the scattered light is proportional to the square of the light scattering particles in solution, the size distributions obtained with DLS are enriched with the big clusters of protofibrils. Indeed, it has been shown previously with both DLS and transmission electron microscopy that Sso AcP protofibrils tend to associate together and form big clusters (69).

The observed kinetic profiles of far-UV CD, light scattering and ThT fluorescence have several implications. First, the lower TFE concentrations used here for the three mutants relative to the wild-type protein do not *per se* inhibit aggregation, as an increase of ThT fluorescence is observed in all cases. Second, the mutants aggregate into ThT-binding protofibrils, but do not form transiently native-like assemblies. In other words, the conditions used here promote aggregation of the mutants, but this occurs via a different pathway as protofibril formation is not preceded by accumulation of native-like assemblies. While the first and second phases of aggregation for wild-type Sso AcP in 20% TFE are both faster than unfolding under the same conditions, the ThT fluorescence kinetics of the mutants in 3% or 10% TFE are much slower than unfolding under the same conditions (compare $k_{F-U}^{H_2O}$ and k_2^{ThT} values in Table 5.4). This suggests that aggregation of the mutants may occur via unfolding. Third, despite all mutants in their respective TFE concentrations are remarkably less stable than the wild-type protein in 20% TFE (Table 5.4), formation of ThT-binding protofibrils is slower for the mutants. The first and second phases of

aggregation were previously found to correlate inversely with the conformational stability of the folded state in a group of Sso AcP variants. The trend observed here is opposite, with the destabilised variants forming the protofibrils more slowly and not forming the native-like aggregates at all. This rules out that the changes of aggregation behavior observed for the mutants arise from the different conditions employed.

5.5 Discussion

Amyloid fibril formation is a complex process in which the initial steps consist in the formation of aggregates that can reorganize or assemble further into other species, until critical nuclei are formed to trigger fibril elongation (17). The detailed investigation of the early steps of aggregation by folded proteins is revealing that such proteins can aggregate either following their unfolding into fully or partially unfolded states or via the assembly of protein molecules in their native or native-like state that subsequently can reorganize into β-sheet containing species. Both pathways have been observed within the acylphosphatase-like structural family, providing a very favorable opportunity to explore the determinants of either process through a comparative analysis of the structural characteristics of the proteins involved.

The two members following the "native-like aggregation pathway" (Sso AcP and AcPDro2) differ from the two proteins aggregating via the unfolding route (mAcP and HypF-N) for their higher content of residues in an unfolded structure and for the paucity of protections present at the edge strands of the

native β-sheet. A protein engineering approach has shown that the unstructured N-terminus and the edge β-strand 4 play a key role in the formation of the native-like aggregates by Sso AcP (78). It was previously shown that it is possible to inhibit the formation of the native-like aggregates of Sso AcP by decreasing the unfolded content of the native state, i.e. by removing the unstructured N-terminus (78). This work has shown that the same effect can be achieved by introducing structural protections at edge β-strand-4. This results in the suppression, or retardation, of the formation of the later protofibrils, as these have to form through an alternative pathway that probably proceeds following denaturation. It will be important to extend these approaches to other structural families, in an attempt to delineate more broadly the factors governing the early steps of a process as fundamental as amyloid formation.

CHAPTER VI - CONCLUSIONS

The results presented in this thesis provide insight into the phenomenon of native-like aggregation, that is the process by which proteins convert from their native states into amyloid-like fibrils or their intermediate oligomers without unfolding across the major free energy barrier of unfolding.

The biophysical characterization performed on AcPDro2 aggregation under conditions in which the protein is initially native has confirmed the existence of an aggregation mechanism that is not consistent with the "conformational change hypothesis", based on the concept that a protein with a well defined three-dimensional fold needs to unfold to initiate aggregation. AcPDro2 forms amyloid-like fibrils under conditions in which the protein is not just initially native, but even has a conformational stability similar to that measured under conditions in which aggregation dos not occur. Kinetic tests have then showed that the observed aggregation rate cannot be explained using a model in which the native state unfolds and then aggregates.

It is important to point out that this finding does not contradict the notion that many other proteins need to unfold, at least partially, to form amyloid-like structures. The fact remains that the fully or partially unfolded states that are populated following biosynthesis on the ribosome, stress conditions or mutation are the conformational states that are most susceptible to initiate aggregation. Nevertheless, folded proteins spend most of their lifetime in a folded rather than unfolded state. In some of these diseases the

residual propensity of folded states to aggregate, albeit much lower than that of unfolded states, can become significant under physiological conditions, especially when considering that amyloid formation is extremely slow even in the most aggressive manifestations of protein deposition diseases.

Following the observation of amyloid fibril formation via a mechanism of native-like aggregation in AcPDro2, which adds to the previous finding that Sso AcP forms amyloid-like protofibrils through a similar mechanism, the aggregation processes of these two protein systems were investigated in the presence of a physiological ligand to act as an inhibitor of aggregation. As mentioned in Chapter 1.5, addition of a ligand binding specifically to the native structure of a protein inhibits aggregation when full or partial unfolding is required to initiate aggregation. Here it was shown that ligands also inhibit amyloid formation when the process does not require unfolding as an initial step, but assembly into native-like structures that later convert into amyloid structures. This indicates that the structure-based design of ligands binding with high affinity to the native soluble state of an amyloidogenic protein can be a universal therapeutic strategy to inhibit amyloid formation in pathological states. This therapeutic approach can be effective not just because it is independent of the aggregation pathway, but also because it interferes with the thermodynamics and kinetics of the very early steps of the aggregation process, therefore resulting in the inhibition of any early oligomeric species including native-like oligomers, that are increasingly thought to be pathogenic species in many protein deposition diseases.

Finally, the process of native-like aggregation was explored at a molecular level. Taking advantage of the finding that members of the

acylphosphatase-like structural family aggregate via native-like aggregation or unfolding-based processes, depending on the specific case, the native structures of the various proteins were compared with the aim of identifying the determinants of either pathway. Subtle but interesting structural differences were found between AcPs following the "native-like" pathway and the other AcPs aggregating via the "unfolding" pathway. The former were shown to possess a higher percentage of unordered structure and a lower extent of structural protection at the edge β-strands. A mutational study targeted on the edge β-strand-4 of SsoAcP and aimed at introducing specific structural protection against aggregation phenomena propagating from it has demonstrated that is possible to influence the aggregation rate of a protein by introducing protective structural features and shift the aggregation pathway towards the formation of an unfolded intermediate.

It will be interesting to clarify wheter native-like aggregation is the effective process occurring *in vivo* and causing protein deposition diseases and investigate further such a process at a molecular level to elucidate its general determinants.

REFERENCES

1. Anfisen, C. B. (1973) *Science* **181**, 223-230
2. Dobson, C. M., Sali, A., and Karplus, M. (1998) *Angew. Chem. Int. Ed. Eng.* **37**, 868-893
3. Dill, K. A., and Chan, H. S. (1997) *Nat Struct Biol* **4**(1), 10-19
4. Dobson, C. M. (2003) *Nature* **426**(6968), 884-890
5. Wolynes, P. G., Onuchic, J. N., and Thirumalai, D. (1995) *Science* **267**(5204), 1619-1620
6. Dinner, A. R., Sali, A., Smith, L. J., Dobson, C. M., and Karplus, M. (2000) *Trends Biochem Sci* **25**(7), 331-339
7. Ellis, R. J. (2001) *Curr Opin Struct Biol* **11**(1), 114-119
8. Hartl, F. U., and Hayer-Hartl, M. (2002) *Science* **295**(5561), 1852-1858
9. Schiene, C., and Fischer, G. (2000) *Curr Opin Struct Biol* **10**(1), 40-45
10. Sitia, R., and Braakman, I. (2003) *Nature* **426**(6968), 891-894
11. Keller, J. N., Hanni, K. B., and Markesbery, W. R. (2000) *J Neurochem* **75**(1), 436-439
12. McNaught, K. S., and Jenner, P. (2001) *Neurosci Lett* **297**(3), 191-194
13. Cheung, J. C., and Deber, C. M. (2008) *Biochemistry* **47**(6), 1465-1473
14. Amaral, M. D. (2004) *J Mol Neurosci* **23**(1-2), 41-48
15. Thomas, P. J., Qu, B. H., and Pedersen, P. L. (1995) *Trends Biochem Sci* **20**(11), 456-459
16. Lomas, D. A., and Carrell, R. W. (2002) *Nat Rev Genet* **3**(10), 759-768
17. Chiti, F., and Dobson, C. M. (2006) *Annu Rev Biochem* **75**, 333-366
18. Berriman, J., Serpell, L. C., Oberg, K. A., Fink, A. L., Goedert, M., and Crowther, R. A. (2003) *Proc Natl Acad Sci U S A* **100**(15), 9034-9038
19. Serpell, L. C., Berriman, J., Jakes, R., Goedert, M., and Crowther, R. A. (2000) *Proc Natl Acad Sci U S A* **97**(9), 4897-4902
20. Hoang, T. X., Marsella, L., Trovato, A., Seno, F., Banavar, J. R., and Maritan, A. (2006) *Proc Natl Acad Sci U S A* **103**(18), 6883-6888

21. Uversky, V. N., and Fink, A. L. (2004) *Biochim Biophys Acta* **1698**(2), 131-153
22. Serpell, L. C., Sunde, M., Benson, M. D., Tennent, G. A., Pepys, M. B., and Fraser, P. E. (2000) *J Mol Biol* **300**(5), 1033-1039
23. Sunde, M., and Blake, C. (1997) *Adv Protein Chem* **50**, 123-159
24. Harper, J. D., Wong, S. S., Lieber, C. M., and Lansbury, P. T. (1997) *Chem Biol* **4**(2), 119-125
25. Serpell, L. C. (2000) *Biochim Biophys Acta* **1502**(1), 16-30
26. Walsh, D. M., Hartley, D. M., Kusumoto, Y., Fezoui, Y., Condron, M. M., Lomakin, A., Benedek, G. B., Selkoe, D. J., and Teplow, D. B. (1999) *J Biol Chem* **274**(36), 25945-25952
27. Harper, J. D., Lieber, C. M., and Lansbury, P. T., Jr. (1997) *Chem Biol* **4**(12), 951-959
28. Ivanova, M. I., Gingery, M., Whitson, L. J., and Eisenberg, D. (2003) *Biochemistry* **42**(46), 13536-13540
29. Jaroniec, C. P., MacPhee, C. E., Astrof, N. S., Dobson, C. M., and Griffin, R. G. (2002) *Proc Natl Acad Sci U S A* **99**(26), 16748-16753
30. Petkova, A. T., Ishii, Y., Balbach, J. J., Antzutkin, O. N., Leapman, R. D., Delaglio, F., and Tycko, R. (2002) *Proc Natl Acad Sci U S A* **99**(26), 16742-16747
31. Ritter, C., Maddelein, M. L., Siemer, A. B., Luhrs, T., Ernst, M., Meier, B. H., Saupe, S. J., and Riek, R. (2005) *Nature* **435**(7043), 844-848
32. Makin, O. S., Atkins, E., Sikorski, P., Johansson, J., and Serpell, L. C. (2005) *Proc Natl Acad Sci U S A* **102**(2), 315-320
33. Nelson, R., Sawaya, M. R., Balbirnie, M., Madsen, A. O., Riekel, C., Grothe, R., and Eisenberg, D. (2005) *Nature* **435**(7043), 773-778
34. Dobson, C. M. (1999) *Trends Biochem Sci* **24**(9), 329-332
35. Chiti, F., Webster, P., Taddei, N., Clark, A., Stefani, M., Ramponi, G., and Dobson, C. M. (1999) *Proc Natl Acad Sci U S A* **96**(7), 3590-3594
36. De Felice, F. G., Vieira, M. N., Meirelles, M. N., Morozova-Roche, L. A., Dobson, C. M., and Ferreira, S. T. (2004) *Faseb J* **18**(10), 1099-1101
37. Fandrich, M., Fletcher, M. A., and Dobson, C. M. (2001) *Nature* **410**(6825), 165-166

38. Guijarro, J. I., Sunde, M., Jones, J. A., Campbell, I. D., and Dobson, C. M. (1998) *Proc Natl Acad Sci U S A* **95**(8), 4224-4228
39. Sicorello, A., Torrassa, S., Soldi, G., Gianni, S., Travaglini-Allocatelli, C., Taddei, N., Relini, A., and Chiti, F. (2009) *Biophys. J.* **in press**
40. Calloni, G., Zoffoli, S., Stefani, M., Dobson, C. M., and Chiti, F. (2005) *J Biol Chem* **280**(11), 10607-10613
41. Lopez de la Paz, M., de Mori, G. M., Serrano, L., and Colombo, G. (2005) *J Mol Biol* **349**(3), 583-596
42. Tartaglia, G. G., Cavalli, A., Pellarin, R., and Caflisch, A. (2004) *Protein Sci* **13**(7), 1939-1941
43. Ventura, S., Zurdo, J., Narayanan, S., Parreno, M., Mangues, R., Reif, B., Chiti, F., Giannoni, E., Dobson, C. M., Aviles, F. X., and Serrano, L. (2004) *Proc Natl Acad Sci U S A* **101**(19), 7258-7263
44. Wang, W., and Hecht, M. H. (2002) *Proc Natl Acad Sci U S A* **99**(5), 2760-2765
45. Fernandez, A., Kardos, J., Scott, L. R., Goto, Y., and Berry, R. S. (2003) *Proc Natl Acad Sci U S A* **100**(11), 6446-6451
46. West, M. W., Wang, W., Patterson, J., Mancias, J. D., Beasley, J. R., and Hecht, M. H. (1999) *Proc Natl Acad Sci U S A* **96**(20), 11211-11216
47. Chiti, F., Stefani, M., Taddei, N., Ramponi, G., and Dobson, C. M. (2003) *Nature* **424**(6950), 805-808
48. DuBay, K. F., Pawar, A. P., Chiti, F., Zurdo, J., Dobson, C. M., and Vendruscolo, M. (2004) *J Mol Biol* **341**(5), 1317-1326
49. Fernandez-Escamilla, A. M., Rousseau, F., Schymkowitz, J., and Serrano, L. (2004) *Nat Biotechnol* **22**(10), 1302-1306
50. Trovato, A., Chiti, F., Maritan, A., and Seno, F. (2006) *PLoS Comput Biol* **2**(12), e170
51. Zurdo, J., Guijarro, J. I., Jimenez, J. L., Saibil, H. R., and Dobson, C. M. (2001) *J Mol Biol* **311**(2), 325-340
52. Naiki, H., Hashimoto, N., Suzuki, S., Kimura, H., Nakakuki, K., and Gejyo, F. (1997) *Amyloid* **4**, 223-232

53. Serio, T. R., Cashikar, A. G., Kowal, A. S., Sawicki, G. J., Moslehi, J. J., Serpell, L., Arnsdorf, M. F., and Lindquist, S. L. (2000) *Science* **289**(5483), 1317-1321
54. Uversky, V. N., Li, J., Souillac, P., Millett, I. S., Doniach, S., Jakes, R., Goedert, M., and Fink, A. L. (2002) *J Biol Chem* **277**(14), 11970-11978
55. Fezoui, Y., and Teplow, D. B. (2002) *J Biol Chem* **277**(40), 36948-36954
56. Pedersen, J. S., Christensen, G., and Otzen, D. E. (2004) *J Mol Biol* **341**(2), 575-588
57. Bemporad, F., Calloni, G., Campioni, S., Plakoutsi, G., Taddei, N., and Chiti, F. (2006) *Acc Chem Res* **39**(9), 620-627
58. Glabe, C. G. (2008) *J Biol Chem* **283**(44), 29639-29643
59. Kodali, R., and Wetzel, R. (2007) *Curr Opin Struct Biol* **17**(1), 48-57
60. Walsh, D. M., and Selkoe, D. J. (2004) *Protein Pept Lett* **11**(3), 213-228
61. Walsh, D. M., and Selkoe, D. J. (2007) *J Neurochem* **101**(5), 1172-1184
62. Goldberg, M. S., and Lansbury, P. T., Jr. (2000) *Nat Cell Biol* **2**(7), E115-119
63. Stefani, M., and Dobson, C. M. (2003) *J Mol Med* **81**(11), 678-699
64. Kayed, R., Sokolov, Y., Edmonds, B., McIntire, T. M., Milton, S. C., Hall, J. E., and Glabe, C. G. (2004) *J Biol Chem* **279**(45), 46363-46366
65. Ionescu-Zanetti, C., Khurana, R., Gillespie, J. R., Petrick, J. S., Trabachino, L. C., Minert, L. J., Carter, S. A., and Fink, A. L. (1999) *Proc Natl Acad Sci U S A* **96**(23), 13175-13179
66. Quintas, A., Vaz, D. C., Cardoso, I., Saraiva, M. J., and Brito, R. M. (2001) *J Biol Chem* **276**(29), 27207-27213
67. Conway, K. A., Harper, J. D., and Lansbury, P. T., Jr. (2000) *Biochemistry* **39**(10), 2552-2563
68. Gosal, W. S., Morten, I. J., Hewitt, E. W., Smith, D. A., Thomson, N. H., and Radford, S. E. (2005) *J Mol Biol* **351**(4), 850-864
69. Plakoutsi, G., Taddei, N., Stefani, M., and Chiti, F. (2004) *J Biol Chem* **279**(14), 14111-14119
70. Campioni, S., Mossuto, M. F., Torrassa, S., Calloni, G., de Laureto, P. P., Relini, A., Fontana, A., and Chiti, F. (2008) *J Mol Biol* **379**(3), 554-567

71. Morozova-Roche, L. A., Zamotin, V., Malisauskas, M., Ohman, A., Chertkova, R., Lavrikova, M. A., Kostanyan, I. A., Dolgikh, D. A., and Kirpichnikov, M. P. (2004) *Biochemistry* **43**(30), 9610-9619
72. Kayed, R., Head, E., Thompson, J. L., McIntire, T. M., Milton, S. C., Cotman, C. W., and Glabe, C. G. (2003) *Science* **300**(5618), 486-489
73. Hammarstrom, P., Jiang, X., Hurshman, A. R., Powers, E. T., and Kelly, J. W. (2002) *Proc Natl Acad Sci U S A* **99 Suppl 4**, 16427-16432
74. Heegaard, N. H., Sen, J. W., Kaarsholm, N. C., and Nissen, M. H. (2001) *J Biol Chem* **276**(35), 32657-32662
75. Kelly, J. W. (1998) *Curr Opin Struct Biol* **8**(1), 101-106
76. Marcon, G., Plakoutsi, G., and Chiti, F. (2006) *Methods Enzymol* **413**, 75-91
77. Bouchard, M., Zurdo, J., Nettleton, E. J., Dobson, C. M., and Robinson, C. V. (2000) *Protein Sci* **9**(10), 1960-1967
78. Plakoutsi, G., Bemporad, F., Calamai, M., Taddei, N., Dobson, C. M., and Chiti, F. (2005) *J Mol Biol* **351**(4), 910-922
79. Chiti, F., Taddei, N., Bucciantini, M., White, P., Ramponi, G., and Dobson, C. M. (2000) *Embo J* **19**(7), 1441-1449
80. Ferrao-Gonzales, A. D., Souto, S. O., Silva, J. L., and Foguel, D. (2000) *Proc Natl Acad Sci U S A* **97**(12), 6445-6450
81. Villegas, V., Zurdo, J., Filimonov, V. V., Aviles, F. X., Dobson, C. M., and Serrano, L. (2000) *Protein Sci* **9**(9), 1700-1708
82. Canet, D., Last, A. M., Tito, P., Sunde, M., Spencer, A., Archer, D. B., Redfield, C., Robinson, C. V., and Dobson, C. M. (2002) *Nat Struct Biol* **9**(4), 308-315
83. Hammarstrom, P., Sekijima, Y., White, J. T., Wiseman, R. L., Lim, A., Costello, C. E., Altland, K., Garzuly, F., Budka, H., and Kelly, J. W. (2003) *Biochemistry* **42**(22), 6656-6663
84. Chiti, F., Taddei, N., Stefani, M., Dobson, C. M., and Ramponi, G. (2001) *Protein Sci* **10**(4), 879-886
85. Dumoulin, M., Last, A. M., Desmyter, A., Decanniere, K., Canet, D., Larsson, G., Spencer, A., Archer, D. B., Sasse, J., Muyldermans, S., Wyns, L., Redfield, C., Matagne, A., Robinson, C. V., and Dobson, C. M. (2003) *Nature* **424**(6950), 783-788

86. Miroy, G. J., Lai, Z., Lashuel, H. A., Peterson, S. A., Strang, C., and Kelly, J. W. (1996) *Proc Natl Acad Sci U S A* **93**(26), 15051-15056

87. Ray, S. S., Nowak, R. J., Brown, R. H., Jr., and Lansbury, P. T., Jr. (2005) *Proc Natl Acad Sci U S A* **102**(10), 3639-3644

88. Johnson, S. M., Wiseman, R. L., Sekijima, Y., Green, N. S., Adamski-Werner, S. L., and Kelly, J. W. (2005) *Acc Chem Res* **38**(12), 911-921

89. Plakoutsi, G., Bemporad, F., Monti, M., Pagnozzi, D., Pucci, P., and Chiti, F. (2006) *Structure* **14**(6), 993-1001

90. Bemporad, F., Vannocci, T., Varela, L., Azuaga, A. I., and Chiti, F. (2008) *Biochim Biophys Acta* **1784**(12), 1986-1996

91. Corazza, A., Rosano, C., Pagano, K., Alverdi, V., Esposito, G., Capanni, C., Bemporad, F., Plakoutsi, G., Stefani, M., Chiti, F., Zuccotti, S., Bolognesi, M., and Viglino, P. (2006) *Proteins* **62**(1), 64-79

92. Pastore, A., Saudek, V., Ramponi, G., and Williams, R. J. (1992) *J Mol Biol* **224**(2), 427-440

93. Rosano, C., Zuccotti, S., Bucciantini, M., Stefani, M., Ramponi, G., and Bolognesi, M. (2002) *J Mol Biol* **321**(5), 785-796

94. Zuccotti, S., Rosano, C., Ramazzotti, M., Degl'Innocenti, D., Stefani, M., Manao, G., and Bolognesi, M. (2004) *Acta Crystallogr D Biol Crystallogr* **60**(Pt 6), 1177-1179

95. Stefani, M., Taddei, N., and Ramponi, G. (1997) *Cell Mol Life Sci* **53**(2), 141-151

96. Taddei, N., Chiti, F., Magherini, F., Stefani, M., Thunnissen, M. M., Nordlund, P., and Ramponi, G. (1997) *Biochemistry* **36**(23), 7217-7224

97. Taddei, N., Stefani, M., Magherini, F., Chiti, F., Modesti, A., Raugei, G., and Ramponi, G. (1996) *Biochemistry* **35**(22), 7077-7083

98. Taddei, N., Stefani, M., Vecchi, M., Modesti, A., Raugei, G., Bucciantini, M., Magherini, F., and Ramponi, G. (1994) *Biochim Biophys Acta* **1208**(1), 75-80

99. Thunnissen, M. M., Taddei, N., Liguri, G., Ramponi, G., and Nordlund, P. (1997) *Structure* **5**(1), 69-79

100. Nediani, C., Fiorillo, C., Marchetti, E., Pacini, A., Liguri, G., and Nassi, P. (1996) *J Biol Chem* **271**(32), 19066-19073

101. Giannoni, E., Cirri, P., Paoli, P., Fiaschi, T., Camici, G., Manao, G., Raugei, G., and Ramponi, G. (2000) *Mol Cell Biol Res Commun* **3**(5), 264-270

102. Chiarugi, P., Degl'Innocenti, D., Raugei, G., Fiaschi, T., and Ramponi, G. (1997) *Biochem Biophys Res Commun* **231**(3), 717-721

103. Paoli, P., Camici, G., Manao, G., Giannoni, E., and Ramponi, G. (2000) *Biochem J* **349**(Pt 1), 43-49

104. Taddei, N., Chiti, F., Paoli, P., Fiaschi, T., Bucciantini, M., Stefani, M., Dobson, C. M., and Ramponi, G. (1999) *Biochemistry* **38**(7), 2135-2142

105. van Nuland, N. A., Chiti, F., Taddei, N., Raugei, G., Ramponi, G., and Dobson, C. M. (1998) *J Mol Biol* **283**(4), 883-891

106. Bemporad, F., Capanni, C., Calamai, M., Tutino, M. L., Stefani, M., and Chiti, F. (2004) *Biochemistry* **43**(28), 9116-9126

107. Calloni, G., Taddei, N., Plaxco, K. W., Ramponi, G., Stefani, M., and Chiti, F. (2003) *J Mol Biol* **330**(3), 577-591

108. Parrini, C., Bemporad, F., Baroncelli, A., Gianni, S., Travaglini-Allocatelli, C., Kohn, J. E., Ramazzotti, M., Chiti, F., and Taddei, N. (2008) *J Mol Biol* **379**(5), 1107-1118

109. Taddei, N., Chiti, F., Fiaschi, T., Bucciantini, M., Capanni, C., Stefani, M., Serrano, L., Dobson, C. M., and Ramponi, G. (2000) *J Mol Biol* **300**(3), 633-647

110. Marcon, G., Plakoutsi, G., Canale, C., Relini, A., Taddei, N., Dobson, C. M., Ramponi, G., and Chiti, F. (2005) *J Mol Biol* **347**(2), 323-335

111. Degl'Innocenti, D., Ramazzotti, M., Marzocchini, R., Chiti, F., Raugei, G., and Ramponi, G. (2003) *FEBS Lett* **535**(1-3), 171-174

112. Soldi, G., Bemporad, F., Torrassa, S., Relini, A., Ramazzotti, M., Taddei, N., and Chiti, F. (2005) *Biophys J* **89**(6), 4234-4244

113. Soldi, G., Plakoutsi, G., Taddei, N., and Chiti, F. (2006) *J Med Chem* **49**(20), 6057-6064

114. Soldi, G., Bemporad, F., and Chiti, F. (2008) *J Am Chem Soc* **130**(13), 4295-4302

115. Klunk, W. E., Jacob, R. F., and Mason, R. P. (1999) *Methods Enzymol* **309**, 285-305

116. Klunk, W. E., Pettegrew, J. W., and Abraham, D. J. (1989) *J Histochem Cytochem* **37**(8), 1273-1281
117. Khurana, R., Coleman, C., Ionescu-Zanetti, C., Carter, S. A., Krishna, V., Grover, R. K., Roy, R., and Singh, S. (2005) *J Struct Biol* **151**(3), 229-238
118. Krebs, M. R., Bromley, E. H., and Donald, A. M. (2005) *J Struct Biol* **149**(1), 30-37
119. LeVine, H., 3rd. (1999) *Methods Enzymol* **309**, 274-284
120. Stryer, L. (1965) *J Mol Biol* **13**(2), 482-495
121. Matulis, D., and Lovrien, R. (1998) *Biophys J* **74**(1), 422-429
122. Semisotnov, G. V., Rodionova, N. A., Razgulyaev, O. I., Uversky, V. N., Gripas, A. F., and Gilmanshin, R. I. (1991) *Biopolymers* **31**(1), 119-128
123. Ramponi, G., Treves, C., and Guerritore, A. A. (1966) *Arch Biochem Biophys* **115**(1), 129-135
124. Santoro, M. M., and Bolen, D. W. (1988) *Biochemistry* **27**(21), 8063-8068
125. Jackson, S. E., and Fersht, A. R. (1991) *Biochemistry* **30**(43), 10428-10435
126. Woody, R. W. (1995) *Methods Enzymol* **246**, 34-71
127. Greenfield, N. J. (2006) *Nat Protoc* **1**(6), 2876-2890
128. Johnson, W. C., Jr. (1990) *Proteins* **7**(3), 205-214
129. Relini, A., Torrassa, S., Rolandi, R., Gliozzi, A., Rosano, C., Canale, C., Bolognesi, M., Plakoutsi, G., Bucciantini, M., Chiti, F., and Stefani, M. (2004) *J Mol Biol* **338**(5), 943-957
130. Chow, M. K., Paulson, H. L., and Bottomley, S. P. (2004) *J Mol Biol* **335**(1), 333-341
131. Lindberg, M. J., Tibell, L., and Oliveberg, M. (2002) *Proc Natl Acad Sci U S A* **99**(26), 16607-16612
132. Rochet, J. C., and Lansbury, P. T., Jr. (2000) *Curr Opin Struct Biol* **10**(1), 60-68
133. Chow, M. K., Ellisdon, A. M., Cabrita, L. D., and Bottomley, S. P. (2004) *J Biol Chem* **279**(46), 47643-47651
134. Pieri, A., Magherini, F., Liguri, G., Raugei, G., Taddei, N., Bozzetti, M. P., Cecchi, C., and Ramponi, G. (1998) *FEBS Lett* **433**(3), 205-210
135. Venyaminov, S., and Vassilenko, K. S. (1994) *Anal Biochem* **222**(1), 176-184
136. Ptitsyn, O. B. (1995) *Adv Protein Chem* **47**, 83-229

137. Hamada, D., Chiti, F., Guijarro, J. I., Kataoka, M., Taddei, N., and Dobson, C. M. (2000) *Nat Struct Biol* **7**(1), 58-61

138. Matouschek, A., Kellis, J. T., Jr., Serrano, L., Bycroft, M., and Fersht, A. R. (1990) *Nature* **346**(6283), 440-445

139. Chiti, F., Calamai, M., Taddei, N., Stefani, M., Ramponi, G., and Dobson, C. M. (2002) *Proc Natl Acad Sci U S A* **99 Suppl 4**, 16419-16426

140. McParland, V. J., Kad, N. M., Kalverda, A. P., Brown, A., Kirwin-Jones, P., Hunter, M. G., Sunde, M., and Radford, S. E. (2000) *Biochemistry* **39**(30), 8735-8746

141. Raffen, R., Dieckman, L. J., Szpunar, M., Wunschl, C., Pokkuluri, P. R., Dave, P., Wilkins Stevens, P., Cai, X., Schiffer, M., and Stevens, F. J. (1999) *Protein Sci* **8**(3), 509-517

142. Ramirez-Alvarado, M., Merkel, J. S., and Regan, L. (2000) *Proc Natl Acad Sci U S A* **97**(16), 8979-8984

143. Monti, M., Garolla di Bard, B. L., Calloni, G., Chiti, F., Amoresano, A., Ramponi, G., and Pucci, P. (2004) *J Mol Biol* **336**(1), 253-262

144. Richardson, J. S., and Richardson, D. C. (2002) *Proc Natl Acad Sci U S A* **99**(5), 2754-2759

145. Bousset, L., Thomson, N. H., Radford, S. E., and Melki, R. (2002) *Embo J* **21**(12), 2903-2911

146. Souillac, P. O., Uversky, V. N., and Fink, A. L. (2003) *Biochemistry* **42**(26), 8094-8104

147. Laurine, E., Gregoire, C., Fandrich, M., Engemann, S., Marchal, S., Thion, L., Mohr, M., Monsarrat, B., Michel, B., Dobson, C. M., Wanker, E., Erard, M., and Verdier, J. M. (2003) *J Biol Chem* **278**(51), 51770-51778

148. Sasahara, K., Yagi, H., Naiki, H., and Goto, Y. (2007) *Biochemistry* **46**(11), 3286-3293

149. Sasahara, K., Yagi, H., Naiki, H., and Goto, Y. (2007) *J Mol Biol* **372**(4), 981-991

150. Lian, H. Y., Zhang, H., Zhang, Z. R., Loovers, H. M., Jones, G. W., Rowling, P. J., Itzhaki, L. S., Zhou, J. M., and Perrett, S. (2007) *J Biol Chem* **282**(16), 11931-11940

151. Taddei, N., Modesti, A., Bucciantini, M., Stefani, M., Magherini, F., Vecchi, M., Raugei, G., and Ramponi, G. (1995) *FEBS Lett* **362**(2), 175-179